# A THEORETICAL AND EXPERIMENTAL STUDY OF THE PROPAGATION OF PLANE FINITE AMPLITUDE WAVES IN REAL FLUIDS

Thesis for the Degree of Ph. D.

MICHIGAN STATE UNIVERSITY

William Wright Lester

1963

This is to certify that the

thesis entitled

# A THEORETICAL AND EXPERIMENTAL STUDY OF THE PROPAGATION OF PLANE FINITE AMPLITUDE WAVES IN REAL FLUIDS

presented by

William Wright Lester

has been accepted towards fulfillment
of the requirements for

Ph. D. degree in Physics

E. A. Hiedemann
Major professor

Date November 13, 1963

O-169

ABSTRACT

A THEORETICAL AND EXPERIMENTAL STUDY OF THE PROPAGATION OF PLANE FINITE AMPLITUDE WAVES IN REAL FLUIDS

by William Wright Lester

Longitudinal elastic waves of large amplitude propagated in real fluids exhibit a change in form and amplitude as they travel. An initially sinusoidal plane, finite amplitude wave is of special interest. A theory is presented which predicts the harmonic structure of such a wave on the hypothesis that interactions between harmonic components of the wave are weak compared with the processes which generate and absorb harmonics. The result is given as an infinite sum of infinite series, and is a function of two parameters, one which specifies the initial conditions, and one which specifies the distance of travel in a reduced form. Numerical values of the predicted fundamental, second, and third harmonics are tabulated for general use; the numerical values of the second and third harmonics have been computed for a wide range of the governing parameters. The general behavior of the harmonic structure is as expected from plausible arguments and the results of other investigators.

An experimental investigation making use of pulse techniques in water in conjunction with optical methods

verifies essential aspects of the theory. The accurate transducer calibration required to specify both the initial value and reduced distance parameters of the theory is accomplished by observation of light diffracted by the ultrasonic pulse at the transducer face. Temperature stability of the calibration of barium titanate transducers is demonstrated. The equivalence of the finite amplitude waveform for pulsed and continuous waves of identical frequency and initial pressure amplitude is also demonstrated, so that pulsed and continuous wave methods may be used interchangeably.

An investigation of the behavior of the fundamental frequency component of a finite amplitude wave is performed using a two transducer pulse technique at 5 MC. The behavior of the fundamental frequency component as a function of pressure at fixed distance is obtained, and converted to plots of pressure versus distance at fixed initial pressure. The fixed distance method is found to work best for small values of the initial value parameter. The average and maximum values of the absorption coefficient of the fundamental frequency component of a finite amplitude wave are found to be linear functions of the initial pressure amplitude. A value for the nonlinearity parameter B/A of water is obtained from absorption measurements using weak shock theory. It is found that there is a maximum amount of fundamental sound pressure amplitude which can

be transmitted over a given distance. Distances as large as 50 cm and initial pressure amplitudes to 15 atm are used.

The two transducer pulse technique used to investigate the fundamental frequency component is extended to the case of the second harmonic at 5.0 MC, and is found to perform well for larger values of the initial value parameter in this case. The receiving transducer is calibrated by allowing a finite amplitude wave of previously measured second harmonic content to fall upon it while measuring the output with a tuned receiving system. The absolute measurement of second harmonic content is performed by light diffraction techniques using continuous waves. Light diffraction techniques are also used to verify the theory for the values of the fundamental, second and third harmonics simultaneously for a range of distances for one initial pressure amplitude. Initial pressures as large as 1.9 atm and distances as large as 80 cm are used. Comparison of the second harmonic with the theoretical predictions indicate satisfactory agreement.

# A THEORETICAL AND EXPERIMENTAL STUDY OF THE PROPAGATION OF PLANE FINITE AMPLITUDE WAVES IN REAL FLUIDS

By

William Wright Lester

A THESIS

Submitted to
Michigan State University
in partial fulfillment of the requirements
for the degree of

DOCTOR OF PHILOSOPHY

Department of Physics and Astronomy

1963

ACKNOWLEDGMENT

The author wishes to express his gratitude to Professor E. A. Hiedemann for his guidance in this work. Thanks are also due to Dr. K. L. Zankel, Dr. B. D. Cook, Dr. M. A. Breazeale, and Dr. W. G. Mayer for many interesting and helpful discussions. The financial support of the Office of Naval Research, U. S. Navy, and the U. S. Army Research Office (Durham) is gratefully acknowledged.

TABLE OF CONTENTS

LIST OF TABLES

LIST OF FIGURES

FIGURE PAGE

FIGURE PAGE

## LIST OF SYMBOLS

$C'$ = Velocity of wave phase points.

$C_o$ = Sound velocity for infinitesimal amplitudes.

$P$ = Pressure.

$P_o$ = Internal (equilibrium) pressure.

$\rho$ = Density.

$\rho_o$ = Equilibrium density.

$A$, $B$ = Empirical constants in the equation of state.

$X$ = Distance from origin of wave.

$u$ = Particle velocity.

$\alpha$ = Infinitesimal amplitude absorption coefficient for the fundamental frequency component.

$f(n)$ = Factor by which $\alpha$ must be multiplied in order to obtain the absorption coefficient of the nth harmonic in the medium of interest.

$\omega$ = Fundamental frequency.

$L$ = Discontinuity distance for dissipationless case.

$K=X/L$ = Reduced distance.

$\tilde{K}$ = $10X/L$.

$P_n(K)$ = Pressure amplitude of the nth harmonic wave component, measured at reduced distance K.

$\delta_n(\tilde{K})$ = Harmonic generation parameter (Fox and Wallace).

$\lambda$ = Wavelength.

# CHAPTER I

## INTRODUCTION

For a long time, it has been known that an exact solution to the equations of hydrodynamics predicts a change in form of a longitudinal elastic wave as it travels (1,2,3,4,5). These early theoretical investigations were performed for the simple case of a plane wave in a nondissipative medium, and showed that a simultaneous solution to the nonlinear differential equations of hydrodynamics and the equation of state could be obtained. This solution was in a form such that the value of the propagation velocity of phase points on the wave depended on the pressure-density relation at that point and the local particle velocity. Thus, the usual case is that the points of higher pressure (particle velocity) travel faster than the points of lower pressure, and the wave becomes distorted, or acquires various Fourier frequency components as it travels. These early investigators classified these waves as finite in amplitude, in contrast with the usual case of infinitesimal amplitude waves, because the solutions to the infinitesimal amplitude case were obtained from the equations of hydrodynamics and state by neglecting small quantities of second order, while it was necessary to consider second order quantities in order to show the change

in wave shape one should actually have. Of course, it is never really correct to neglect the second order quantities, so that, strictly speaking, all waves are finite in amplitude. However, if one considers that the medium is dissipative, it can be shown that only waves of large amplitude exhibit the appreciable change in form predicted by the nondissipative theory; the absorptive processes in the medium oppose the generation of higher Fourier components as the wave travels, cancelling the rather weak harmonic generation process in the case of small amplitude waves. Hence, one has the correct division of wave propagation processes in real media into two categories: large and small amplitude. Special interest is drawn to one case since it is easy to investigate and commonly encountered, and that is the case of an initially sinusoidal, large amplitude plane wave in a real (nonlinear, dissipative) fluid.

The more recent theoretical approaches to this problem have been of two general types. First of all, approximation methods making use of some assumption regarding the manner in which the harmonic components of a wave are created and absorbed in the medium have been used (6,7,8). Second, approximate solutions to the nonlinear differential equations have been sought, either by perturbation technique or other means (9-14). In general, these theories predict that an initially sinusoidal wave of finite amplitude

develops a spectrum of higher harmonic Fourier components as it travels, the second harmonic being the most important, and that these higher harmonics first grow rapidly, rising to a maximum at some distance from the source, and then decline slowly. Since the higher Fourier components all come to a maximum in the same neighborhood, and then decrease slowly (as does the fundamental frequency component), one may speak of a region in which the wave shape is comparatively stable, or a "stabilization distance" of travel from the source. The absorption coefficient for a finite amplitude wave is also different from that of a sinusoidal wave. Generally speaking, the absorption loss for a sinusoidal wave travelling in a simple fluid is due to two causes; one, viscosity, and two, heat conduction between the hotter, compressed parts of the wave and the cooler, rarefied parts. Analysis of each of these mechanisms predicts that the losses for such a wave of pure frequency should be proportional to the square of the frequency. In the finite amplitude case, energy must be taken from the fundamental frequency component of the wave in order to support growth of the higher harmonics, and since one expects them to be absorbed much more strongly than the fundamental frequency component, the overall energy loss in the wave per unit of distance may be much greater than in the case of a small amplitude wave, and must also depend on the distance. Likewise, one may speak of a partial

absorption coefficient for a given harmonic component, and it will in general depend on the distance and pressure amplitude of the wave.

Experimental investigations of the propagation of plane, finite amplitude waves have been performed in both gases (6, 15,16) and liquids (7,17-27). Generally speaking, these investigators have made use of either spectral analysis of the waveform or observation of the actual pressure waveshape or intensity as a function of the distance, thereby obtaining the harmonic structure and absorption coefficient of the wave. However, the amount and range of useful experimental data available is still quite small for several reasons. First of all, it must be emphasized that the theoretical problem at hand is an "initial value" problem, that is, at zero distance a sinusoidal wave of known amplitude and frequency is postulated in a medium whose properties are known, and it is the task of the theory to predict what becomes of the wave at other times and distances. It thus becomes the first task of the experimenter to provide an accurate measurement of the waveform amplitude at zero distance; the measurement of the wave frequency and properties of the medium are comparatively easy. Confining our attention for the remainder of the discussion to the case of liquids, measurements of the waveform amplitude have been performed by a number of methods, such as calorimetry (23,17,19), thermal probe receivers (23),

radiometry (23,7), and theoretical transmitter response (27). However, there are many difficulties inherent in these methods. For example, two methods may be used simultaneously and yet give grossly different results (23). Also, it is difficult to make an estimate of absolute error, which is essential if one is to make accurate judgments when comparing results with theory. Again, some methods do not work well at small distances of travel from the sending transducer, forcing extrapolation of pressure versus distance curves to zero distance (7), a very dubious procedure in the finite amplitude case. These problems can all be resolved with the use of optical techniques for absolute pressure measurement.

One very troublesome problem in the case of methods making use of continuous waves is the possibility of stray reflections in the apparatus, giving rise to interferences and standing waves which must be avoided in order to obtain accurate comparison with theory. It is, therefore, advantageous to use pulse methods, so that reflected wave effects can easily be separated in time of arrival from direct wave effects. This introduces the experimental difficulty of making absolute sound pressure measurements of an untrasonic pulse by optical means, but it will presently be seen that this difficulty has been resolved (28).

The choice of liquid which one wishes to perform experiments on will be dictated, apart from considerations

of convenience and safety, by the necessity of knowing as accurately as possible those physical constants of the liquid which appear from the theory to govern finite amplitude wave propagation. An examination of the theory at hand (8) shows that such properties as the absorption coefficient for small amplitude waves, a parameter specifying the mechanical nonlinearity of the medium, and the sound velocity for infinitesimal amplitudes, are needed in an accurate form, as well as other parameters not usually troublesome. These properties are best known and most investigated for water (29-31). The first attempt at verification of the theory was, therefore, made by means of measurements in water.

It will, therefore, be the task of the present dissertation to formulate a theory describing the propagation of plane, finite amplitude waves in a dissipative fluid, and to investigate and tabulate the properties of that solution. In addition, an experimental investigation making use of pulse techniques in conjunction with optical methods in water will be presented as verification of the theory.

# CHAPTER II

## THEORY OF THE PROPAGATION OF PLANE, FINITE AMPLITUDE WAVES

### Fundamental Relations

In general, a plane elastic wave traveling in an infinite, nondissipative fluid exhibits a change in form as it travels. This fact can be seen from the nonlinear form of the equations of motion and state. For example, in Eulerian coordinates one has the equations of motion

$$dP/dx = -\rho\left[(du/dt) + u(du/dx)\right] \tag{1}$$

$$\frac{dp}{dt} + \frac{d}{dx}(\rho u) = 0, \tag{2}$$

the first representing a force law, and the second, the conservation of mass. The adiabatic equation of state may be taken as the series expansion to terms of second order

$$P - P_o = A\left(\frac{\rho - \rho_o}{\rho_o}\right) + \frac{B}{2}\left(\frac{\rho - \rho_o}{\rho_o}\right)^2 \tag{3}$$

or, alternatively, one may use the gas-like equation of state

$$P/P_o = (\rho/\rho_o)^{\gamma} \tag{4}$$

both of which are nonlinear, applicable to the fluid state,

and equivalent under certain conditions. It should be noted that in the case of a gas, $\gamma$ is the ratio of the specific heats Cp/Cv; in the case of a liquid, however, it is an empirical constant.

A solution to Eqs. 1 and 2 has been known in implicit form for some time. Simply stated, any initial wave function F (X) can be propagated in the positive direction with a velocity C', where

$$C' = (dP/d\rho)^{\frac{1}{2}} + u \tag{5}$$

is the velocity of phase points of the wave (4). C' is simply interpreted as the sum of the sound velocity $C = (dP/d\rho)^{\frac{1}{2}}$ and the velocity of the moving medium U at the phase point. The consequences of this are apparent: any function

$$u = F\left[X - \left((dP/d\rho)^{\frac{1}{2}} + u\right) t\right] \tag{6}$$

represents a wave travelling the positive X direction satisfying Eqs. 1 and 2, and since in general $(dP/d\rho)^{\frac{1}{2}} + u > C_o$ for $u > o$, a discontinuity develops in the wave after a certain distance of travel, for the points of greater particle velocity overtake the points of lesser particle velocity. For an initially sinusoidal wave, this distance, the so-called discontinuity distance L, is

$$L = \frac{\rho_o C_o^{\,3}}{\pi(B/A + 2)P_1(o)\gamma} \tag{7}$$

At the distance L, the wave develops an infinite slope at its point of zero particle velocity.

One notes that the group velocity of the wave is unchanged, as the points of zero particle velocity move at the velocity of sound $C_o$, where

$$C_o = \left(dP/d\rho\right)^{\frac{1}{2}}_{u=o} . \tag{8}$$

The wavelength is constant, as the points of zero particle velocity maintain their relative separation as they travel.

The pressure and particle velocity are simply related in a finite amplitude wave, and one can introduce the acoustic impedance $\rho_o C_o$ so that

$$P - P_o = \rho_o C_o u \tag{9}$$

The Phase Velocity of a Plane, Finite Amplitude Wave

Expansion of Eq. 5 in series, making use of Eq. 3 and 9, yields the series in u to terms of second order

$$C' = C_o \left[ 1 + \left(1 + \frac{B}{2A}\right) \frac{u}{Co} - \frac{3}{8} \frac{B^2}{A^2} \left(\frac{u}{C_o}\right)^2 + \ldots \right] \tag{10}$$

where the identification from Eq. 8

$$C_o = \left(A/\rho_o\right)^{\frac{1}{2}} \tag{11}$$

has been made. One may evidently neglect the second order term in u for cases where

$$\left| \frac{\frac{3}{8}\frac{B^2}{A^2}\frac{u}{Co}}{\frac{B}{2A}+1} \right| \ll 1 \qquad (12)$$

In typical liquids, we have $\frac{B}{A} \sim 10$ and $C_o \sim 10^5$ cm/sec, so that

$$\frac{\frac{3}{8}\frac{B^2}{A^2}\frac{u}{Co}}{\frac{B}{2A}+1} \sim \frac{10^{-3}}{16}\, u \qquad (13)$$

Thus, the second order terms in u become comparable with the first order terms for pressures of the order

$$P - P_o \sim \rho_o C_o\ (16 \times 10^3) \sim 16 \times 10^8 \text{ dynes/cm}^2 \qquad (14)$$

that is, for waves of the order of 1600 atmospheres of peak pressure. For waves of considerably less than 1600 atmospheres pressure, one may take as the velocity of phase points of the wave

$$C' = C_o + \left(1 + \frac{B}{2A}\right) u. \qquad (15)$$

If terms in $u^2$ must be included in Eq. 15, the equation of state (3) would probably be inadequate, and a third order term could be included.

A similar calculation, beginning with the alternate equation of state Eq. 4, making use as before of Eqs. 5 and 9, yields

$$C' = C_o + \left(\frac{\gamma + 1}{2}\right)u + \frac{\gamma(\gamma - 1)(\gamma - 3)}{8}\left(\frac{u}{C_o}\right)^2 + \ldots, \quad (16)$$

and one may again neglect second order terms in u if

$$\left|\frac{\gamma(\gamma - 1)(\gamma - 3)\,u}{4(\gamma + 1)\,C_o^2}\right| \ll 1 \quad (17)$$

Supposing for the moment that one is dealing with a gas, take $\gamma \sim 1.5$, and $C_o \sim 3 \times 10^5$ cm/sec, $\rho_o \sim .0012$ g/cc (corresponding roughly to the case of air at atmospheric pressure). Then

$$\left|\frac{\gamma(\gamma - 1)(\gamma - 3)u}{4(\gamma + 1)C_o^2}\right| = \left|\frac{\gamma(\gamma - 1)(\gamma - 3)\,(P - P_o)}{4(\gamma + 1)\rho_o C_o^3}\right| = 1, \quad (18)$$

if

$$P - P_o \sim 1.7 \times 10^{14} \text{ dynes/cm}^2. \quad (19)$$

That is, one may use the expansion for the phase velocity

$$C' = C_o + \left(\frac{\gamma + 1}{2}\right)u \quad (20)$$

in gases at atmospheric pressure if the peak wave pressure is considerably less than $1.7 \times 10^8$ at m.

The equations of state, Eqs. 3 and 4, are both applicable to either gases or liquids, and they are equivalent as far as the propagation of elastic waves is concerned in the approximation that the square of the particle velocity may be neglected. Comparison of Eqs. 15 and 20 shows that one may take

$$\frac{B}{A} + 1 = \gamma \quad . \tag{21}$$

Also, since Eq. 7 follows from the phase velocity Eq. 5 as expanded in Eq. 15, one must have the alternate form for Eq. 7 as follows:

$$L = \frac{\rho_o c_o^3}{\pi(\gamma + 1)P_1(o)\nu} \tag{22}$$

Solution for the Case of a Plane, Initially Sinusoidal Wave

Fubini-Ghiron (32), Keck and Beyer (13), and Hargrove (33) have given a series solution of the finite amplitude problem for the dissipationless case which describes the harmonic wave structure as a function of the distance. This solution, for the case of an initially sinusoidal wave, is given by Hargrove in the form

$$P(K) = 2P_1(0) \sum_{n=1}^{\infty} (-1)^{n+1} \frac{J_n(nK)}{nK} \sin 2\pi n(\nu t - \frac{x}{\lambda}) \tag{23}$$

and is valid only for distances $X \leq L$, i.e., for $K \leq 1$. It should be noted that Eq. 23 is obtained from Eqs. 6, 9, and 15 or 20, and is valid only where these hold. In particular, as has been stated, Eq. 23 should hold in the case of simple liquids for waves of finite amplitude provided $P_1(0) \ll 1600$ at. This result (Eq. 23) allows one to write a Fourier series for the pressure components of an initially sinusoidal wave in a dissipative medium.

In a nondissipative medium, examination of Eq. 23 (see Figs. 1, 2, 3 for $\alpha L = 0$) shows that the wave begins with a pure frequency $\nu$, and develops higher harmonics of frequency $n\nu$ at the expense of the component of frequency $\nu$. Let this mechanism of the shift of pressure from one harmonic to another be called the "transfer" mechanism. Inasmuch as it is a function of the distance, one may write the spatial derivative

$$(dP_n(K)/dK)_{transfer} = 2P_1(0)(-1)^{n+1} \frac{d}{dK}\left[\frac{Jn(nK)}{nK} \sin 2\pi n\left(\nu t - \frac{x}{\lambda}\right)\right] \qquad (24)$$

In the absence of finite amplitude effects, the space rate of change of the pressure due to absorption is simply proportional to the total pressure of a given harmonic. If the absorption mechanism is heat conduction between the hotter, compressed parts of the wave, and the cooler, rarefied parts, or if it is viscosity, the absorption is also proportional to $n^2$. For the sake of generality, let the proportionality for the nth harmonic component be given by f(n). Then

$$(dP_n(K)/dK)_{absorp} = -f(n)\, \alpha L P_n(K)_{total} \qquad (25)$$

The total space rate of change of the amplitude of a harmonic component is now assumed to be the sum of the rates of change due to harmonic transfer and harmonic absorption:

$$(dP_n(K)/dK)_{total} = (dP_n(K)/dK)_{transfer} - f(n)\alpha L P_n(K)_{total} \quad (26)$$

This assumption has first been used successfully by Thuras, Jenkins, and O'Neill (6) for the case of small distance propagation of finite amplitude waves in a gas-filled tube.

Before solving Eq. 26, note that this linear addition leads approximately to the Fox and Wallace relations (7), as is seen on conversion of Eq. 26 to a finite difference relationship. For small K or $\alpha L$, one can assume $(P_n(K)_{transfer}/P_n(K)_{total} \approx 1$, and can rewrite Eq. 26 in the form

$$d(\ln P_n(K)_{total}) = d(\ln P_n(K)_{transfer}) - \alpha f(n)dx. \quad (27)$$

In terms of the intervals proposed by Fox and Wallace, we have

$$P_n(\tilde{K} + 1) = P_n(\tilde{K}) \times \exp\left\{\ln\left[P_n(K + 0.1)/P_n(K)\right]_{transfer} - \alpha f(n)\Delta X\right\}, \quad (28)$$

but

$$\ln\left[P_n(K + 0.1)/P_n(K)\right]_{transfer} = \delta_n(\tilde{K}), \quad (29)$$

as can be verified numerically from Eq. 23 and the graphically determined values from Fox and Wallace, taking into account the change in sign of $\delta_1(\tilde{K})$ which they introduced.

Equation 26 may, therefore, be taken as approximately equivalent to the Fox and Wallace equations, except for the

inclusion of the factor $\exp\left[\delta_1(\tilde{K})\right]$ in their result for the second and third harmonics. Comparison shows, however, that $\delta_1$ is small in comparison with $\delta_2$ or $\delta_3$ for all but the largest K values.

Integration of Eq. 26, using Eq. 24 gives an integral equation of the second kind:

$$P_n(K) = \frac{2P_1(0)J_n(nK)}{nK} - f(n) \alpha L \int_0^K P_n(K')\, dK' \qquad (30)$$

The solution of Eq. 30 by the method of successive substitutions (34) (assuming $\alpha L$ approximately constant) is an infinite alternating series for the nth harmonic amplitude of the form

$$P_n(K) = A_n(K) - B_n(K) + C_n(K) - D_n(K) + E_n(K).....+..... \qquad (31)$$

The first five terms are found to be

$$A_n(K) = 2P_1(0)\, J_n(nK)/nK \qquad (32a)$$

$$B_n(K) = \frac{2P_1(0)f(n)\alpha L}{n^2}\left(\sum_{q=0}^{\infty} 2J_{n+2q}(nK) - J_n(nK)\right) \qquad (32b)$$

$$C_n(K) = \frac{4P_1(0)f^2(n)\alpha^2L^2}{n^3}\sum_{q=1}^{\infty}(2q-1)\, J_{n+2q-1}(nK) \qquad (32c)$$

$$D_n(K) = \frac{8P_1(0)f^3(n)\alpha^3L^3}{n^4}\sum_{q=1}^{\infty} q^2 J_{n+2q}(nK) \qquad (32d)$$

$$E_n(K) = \frac{16P_1(0)f^4(n)\alpha^4L^4}{n^5} \sum_{q=1}^{\infty} q^2 \sum_{r=0}^{\infty} J_{n+2(q+r)+1}(nK) \qquad (32e)$$

The solution is thus expressible as the series

$$P(K) = \sum_{n=1}^{\infty} (-1)^{n+1} P_n(K) \sin 2\pi n \left(\nu t - \frac{x}{\lambda}\right), \qquad (33)$$

where the $P_n(K)$ are the harmonic amplitudes given by Eqs. 31 and 32. We must take note of the fact that, as Eq. 23 holds only for $K \leq 1$, Eq. 33 also holds only in this region. For constant $\alpha L$, the series Eqs. 31 and 32 converge absolutely and uniformly in $K \leq 1$.

Terms following those given in Eqs. 32 may be obtained by successively multiplying Eq. 32e by $-2f(n)\alpha L/n$, adding 2s+1 to the order of the Bessel function, and summing over s from zero to infinity. As expected, the correction terms in Eqs. 32 are seen to cause the predicted pressure in any harmonic to be less for a given K value than that predicted by Eq. 23.

## Discussion

For a given absorption law f(n) and reduced distance, the solution is evidently a function only of the product $\alpha L$. Graphs of Eq. 31 for the fundamental, second and third harmonic amplitudes are given in Figures 1, 2, and 3, with the curves from Eq. 23 (dissipationless) for comparison.

The $\alpha L$ values specified for the figures are 0.185 and 0.370. This corresponds to $P_1(0) = 1.0$ and 0.5 atm, respectively, in the case of water at a frequency of 5 Mc/sec, taking $f(n) = n^2$ and $(B/A) = 5$; this value of B/A is given by Beyer (31) for T = 20°C. The dependence of the harmonics on distance is that which one would expect; the second and third harmonics cease growing at about the same K value and decrease slowly at larger K values, which suggests the phenomenon of "waveform stabilization."

Tabulated values of the solution are presented in Tables I, II, and III for the case of the fundamental, second, and third harmonics. The series has been evaluated on the assumption that $f(n) = n^2$, that is, a simple non-relaxing fluid whose losses are proportional to the square of the frequency is considered.

A comparison of the results of the present theory with those of the Fox and Wallace theory has been made for the fundamental and second harmonic frequency components. The fundamental frequency component, as calculated from the Fox and Wallace theory (7) with constant $\Delta X$, yields graphs which very nearly coincide with the curves of Fig. 1, the greatest discrepancy being only $\Delta P_1(K) = 0.02$, or 3%, at $K = 1$ for $\alpha L = 0.370$. In the case of the second harmonic, calculations have been made from the Fox and Wallace theory by assuming the dissipationless value for $P_2(0.1)$ from Eq. 23 and then calculating forward with Eq. 28 for constant $\Delta X$.

TABLE I

FUNDAMENTAL FREQUENCY COMPONENT OF A PLANE,
FINITE AMPLITUDE WAVE $P_1(K)/P_1(0)$

| | K=.1 | .2 | .3 | .4 | .5 | .6 | .7 | .8 | .9 | 1.0 |
|---|---|---|---|---|---|---|---|---|---|---|
| $\alpha L = 0$ | | 1.0 | .99 | .98 | .97 | .96 | .94 | .92 | .90 | .88 |
| $= .185$ | | .96 | .93 | .91 | .88 | .85 | .82 | .79 | .75 | .72 |
| $= .370$ | | .92 | .88 | .84 | .80 | .76 | .72 | .67 | .63 | .58 |

TABLE II

SECOND HARMONIC COMPONENT OF A PLANE, FINITE AMPLITUDE WAVE $P_2(K)/P_1(0)$

| | K = .1 | .2 | .3 | .4 | .5 | .6 | .7 | .8 | .9 | 1.0 |
|---|---|---|---|---|---|---|---|---|---|---|
| $\alpha L = 0$ | .050 | .099 | .146 | .189 | .230 | .265 | .296 | .321 | .340 | .353 |
| .010 | .050 | .098 | .145 | .188 | .227 | .262 | .292 | .316 | .333 | .344 |
| .050 | .049 | .097 | .141 | .182 | .218 | .249 | .275 | .294 | .307 | .313 |
| .100 | .049 | .095 | .137 | .175 | .207 | .234 | .255 | .270 | .278 | .279 |
| .150 | .048 | .093 | .133 | .168 | .197 | .220 | .237 | .248 | .252 | .249 |
| .200 | .048 | .091 | .129 | .161 | .188 | .208 | .221 | .228 | .229 | .223 |
| .250 | .047 | .089 | .125 | .155 | .179 | .196 | .206 | .210 | .208 | .201 |
| .300 | .047 | .088 | .122 | .150 | .171 | .185 | .193 | .195 | .190 | .185 |
| .350 | .046 | .086 | .118 | .144 | .163 | .175 | .180 | .180 | .174 | .164 |
| .400 | .046 | .084 | .115 | .139 | .155 | .165 | .169 | .167 | .160 | .148 |
| .450 | .046 | .083 | .112 | .134 | .149 | .157 | .159 | .156 | .147 | .133 |
| .500 | .045 | .081 | .109 | .129 | .142 | .149 | .149 | .145 | .136 | .123 |
| .550 | .045 | .080 | .106 | .125 | .136 | .141 | .141 | .135 | .125 | .113 |
| .600 | .044 | .078 | .103 | .120 | .130 | .134 | .133 | .127 | .116 | .104 |
| .650 | .044 | .077 | .100 | .116 | .125 | .128 | .125 | .119 | .108 | .096 |
| .700 | .043 | .075 | .098 | .112 | .120 | .122 | .119 | .111 | .101 | .088 |
| .750 | .043 | .074 | .095 | .109 | .115 | .116 | .112 | .105 | .094 | .082 |
| .800 | .043 | .073 | .093 | .105 | .111 | .111 | .106 | .099 | .088 | .076 |
| .850 | .042 | .071 | .091 | .102 | .106 | .106 | .101 | .093 | .082 | .070 |
| .900 | .042 | .070 | .088 | .098 | .103 | .102 | .096 | .088 | .077 | .064 |
| .950 | .041 | .069 | .086 | .095 | .099 | .097 | .091 | .083 | .072 | .059 |
| .990 | .041 | .068 | .084 | .093 | .096 | .094 | .088 | .079 | .068 | .053 |

TABLE III

THIRD HARMONIC COMPONENT OF A PLANE, FINITE AMPLITUDE WAVE $P_3(K)/P_1(0)$

| | K = .1 | .2 | .3 | .4 | .5 | .6 | .7 | .8 | .9 | 1.0 |
|---|---|---|---|---|---|---|---|---|---|---|
| $\alpha L = 0$ | | .015 | .032 | .055 | .081 | .110 | .138 | .165 | .188 | .206 |
| .010 | .004 | .015 | .032 | .054 | .080 | .108 | .135 | .161 | .182 | .198 |
| .050 | .004 | .014 | .031 | .052 | .075 | .100 | .123 | .144 | .160 | .171 |
| .100 | .004 | .014 | .029 | .049 | .070 | .091 | .110 | .127 | .138 | .143 |
| .150 | .004 | .013 | .028 | .046 | .065 | .083 | .100 | .112 | .119 | .120 |
| .200 | .004 | .013 | .027 | .043 | .060 | .077 | .090 | .100 | .104 | .098 |
| .250 | .003 | .013 | .026 | .041 | .057 | .071 | .082 | .089 | .092 | .086 |
| .300 | .003 | .012 | .025 | .039 | .053 | .065 | .075 | .081 | .082 | .070 |
| .350 | .003 | .012 | .024 | .037 | .050 | .061 | .069 | .073 | .073 | .054 |
| .400 | .003 | .012 | .023 | .035 | .047 | .057 | .063 | .067 | .066 | .036 |
| .450 | .003 | .011 | .022 | .034 | .044 | .053 | .059 | .061 | .059 | .013 |

The results for the cases $\alpha L = 0.185$ and $0.370$ are shown in Fig. 4. The Fox and Wallace curves are seen to follow the curves of Fig. 2 up to K values of about 0.6 and 0.4, respectively, and then lie below them, but maintain the same general shape. The discrepancies between the Fox and Wallace theory and the present theory increase with K and $\alpha L$, as expected from the approximation in Eq.27 relating the two theories.

The perturbation analysis of Keck and Beyer (13) also yields functions of the product $\alpha L$ and of the reduced distance K. A calculation of the second harmonic from their result for the cases $\alpha L = 0.185$ and $0.370$ is shown in Fig. 4. It is evident that there is fairly good agreement between the present calculation and their results, with the discrepancy increasing as $\alpha L$ increases.

There remains some question concerning the exact interpretation of the reduced variable K. For the dissipationless case, the value of X corresponding to a given K value is computed on the basis of the initial fundamental pressure. It might equally well be regarded as based on a fundamental pressure component which varies with distance in the manner predicted by Eq. 23. On this interpretation, one may expect the K(X) relationship to depart from linearity as the fundamental frequency component of the pressure is absorbed, and the degree of departure could be estimated numerically. The dependence of the harmonic pressure on

distance would then become a more complicated function than Eq. 33 as the value of L to be used in Eq. 32 would be regarded as a function of the distance.

# CHAPTER III

# AN EXPERIMENTAL STUDY OF THE PROPAGATION OF PLANE, FINITE AMPLITUDE WAVES

## Pulse-Optical Methods

Introduction. The diffraction of light by continuous ultrasonic waves can be used for the absolute measurement of sound-pressure amplitudes (35,36) and for studying the distortion of ultrasonic waves of finite amplitudes (37-39). It is desirable to extend these optical methods to ultrasonic pulses. The evaluation of the experimental results of the optical measurements is based on the Raman-Nath theory (40). This theory predicts the intensity distribution over the diffraction orders as a function of continuous sound-pressure amplitudes. Application of the Raman-Nath theory to the case of ultrasonic pulses would predict that the average relative light intensity distribution over the diffraction orders, except the central order, should be the same as for continuous waves. The absolute average light intensity in these orders would, of course, depend on pulse length and repetition rate. If one can obtain experimental conditions for which the Raman-Nath theory can be applied for ultrasonic pulses, one can use the optical methods previously described for continuous waves. A detailed

experimental investigation is needed in order to evaluate the required experimental conditions.

Cilesiz (41) has made use of a pulse-optical method in which the total instantaneous diffracted light intensity was measured in a limited region in order to obtain relative sound intensities. However, for ultrasonic waveform studies it is necessary to make measurements of the light intensities in discrete diffraction orders. This procedure is also preferable for absolute sound pressure measurements.

The experimental apparatus used in the optical measurements is shown schematically in Fig. 5. The light source S illuminates a slit SL which is used as a source to give a collimated light beam by means of the lens $L_2$. The collimated light beam passes through a rectangular limiting aperture A placed before the ultrasonic beam, and becomes phase modulated by the ultrasonic waves, giving rise to a diffraction pattern consisting of parallel slit images which are brought to a focus by lens $L_3$. The intensities of the diffraction orders are measured by a photomultiplier microphotometer mounted on a laterally traversing micrometer screw.

The Raman-Nath theory predicts that the nth order of diffraction in such an experiment will occur at an angle $\theta_n$ which satisfies $\sin\theta_n = \pm n \lambda / \lambda^*$, where $\lambda$ and $\lambda^*$ are the wavelengths of light and sound, respectively, and n is an integer. The light intensity in the nth diffraction

order is predicted to be $J_n^2(v)$ by this theory. $J_n$ is the nth order Bessel function and $v = 2\pi\mu l/\lambda$, where $\mu$ is the maximum change in index of refraction brought about by the wave and l is the length of the light path in the ultrasonic field. A convenient means of calibration is to observe the maxima or minima of a given diffraction order, and make use of the relationship thus obtained between the Raman-Nath parameter v and the applied voltage. Then from the piezo-optic coefficient relating the change in index of refraction and sound pressure, one can find a pressure-voltage relation. In water, one finds that the acoustic pressure in atmosphere is numerically equal to 0.56 v/l, where l is measured in cm.(38) The possible error of this relation for absolute measurements is estimated to be from 8% to 16% by various sources (35,36) because of the lack of accurate knowledge of the piezo-optic coefficient of water.

The same apparatus can be used for ultrasonic pulses if the time average light intensity of a given diffraction order--except the zero order--is measured. This requires the use of a pulse of nearly rectangular envelope, so that a constant value of the Raman-Nath parameter v would be maintained for approximately the duration of the pulse. Then the time average light intensity observed in a given diffraction order would be that observed in the same order for continuous waves, but reduced by a factor approximately

equal to the fraction of the time that the pulser is on.

The observation of the average light intensity in a given order requires that reflected pulses which can produce diffraction be eliminated. This has been accomplished in the present apparatus by the use of a nonreflecting tank with an absorbing termination of castor oil. The tank is very similar to one described elsewhere (39).

Procedure. A block diagram of the electronic apparatus is shown in Fig. 6. A continuous oscillator or a pulsed oscillator, each with variable output power, may be chosen by a switch. A tuned autotransformer provides impedance matching between the transducer and the pulser. The frequency of the continuous oscillator and the pulser carrier frequency are set to coincidence by means of the heterodyne voltmeter. The voltage and waveform applied to the transducer may be observed on the oscilloscope.

In operation, the pulser frequency is set to the resonant frequency of the transducer, and the frequency of the continuous oscillator is set to coincide with the pulser frequency. The optical system, photomultiplier traversing screw, and transducer are then aligned with continuous waves, and the transducer may be calibrated by observing the voltage required to produce a maximum or minimum in a given diffraction order as observed on the microphotometer. The pulser is then connected to the

transducer and the maxima of the various diffraction orders may be observed. The minima of the orders were less convenient to observe in the present experiment because of the low light levels being measured.

Calibration of a transducer. As an example of the usefulness of the method, a 1/2-inch round nominal 5 Mc transducer of the barium titanate type has been calibrated at 5.45 Mc over the temperature range 5° -33°C in water (42). Because of the known variation of the physical properties of such ceramic transducers, there is some reason to suspect a variation of the calibration with temperature (43). This would limit the usefulness of such transducers for research involving the calibration if such variation had a large slope near room temperature. Figure 7 shows the Raman-Nath parameter v per peak-to-peak volt near the transducer face from pulse and continuous wave measurements on the zero, first, and second orders of diffration. The crosses were obtained as averages of several measurements on the plus and minus second orders of diffraction. A typical set of data for the pulse measurements has a probable error of 3%; the error flag shown is for a possible error of 6%.

For comparison, the triangular data points were obtained using continuous waves, and are seen to lead to approximately the same calibration as was obtained with pulses for this transducer. It should be noted that the

continuous wave measurements, especially at low temperatures, were hindered by heating and streaming effects which made precise measurements difficult; this problem was not present in the pulsed case because of the low average input power.

It can be seen from Fig. 7 that the transducer calibration at fixed frequency varies by only about 12% over a 30°C temperature range for this transducer. The pressure, in atmospheres, is numerically equal to 0.45 v, so that this transducer has a calibrated response of about 0.060 atm per peak-to-peak volt.

A 1/2-inch square 5 Mc transducer of the barium titanate type has also been calibrated. It is found to yield the same calibration with 12 $\mu$ sec pulses as with continuous waves (at 26°C), as was the case with a round transducer.

It remained to be shown that the time average light intensity observed is produced, within negligible error, by the flat topped portion of the pulse, and that no appreciable error is made in neglecting the finite length of the pulse. Accordingly, the dependence of the pulse calibration on pulse length has been observed. Three typical pulses observed on the oscilloscope are shown in Fig. 8. The height in each case corresponds to the peak-to-peak voltage required to produce a first maximum in the first diffraction order. The longest pulse is approximately 10 $\mu$ sec, and the shortest is 3 $\mu$ sec in length. It was found that the calibration was

independent of pulse length until the pulse ceased to be rectangular, which occurred for a pulse length of 3 $\mu$ sec as shown. The failure of the calibration procedure for pulses 3 $\mu$ sec and less in duration is attributable to two causes; the pulse no longer has the rectangular shape suitable for the averaging process, and the limiting light beam aperture was 4.3 mm wide, which corresponds to a time of travel in water of approximately 3 $\mu$ sec. Hence, at a total pulse duration of 3 $\mu$ sec, the limiting aperture width was equal to the pulse length, and the usual diffraction situation ceased to exist.

The instantaneous diffracted light intensity in the first diffraction order has also been observed. A typical oscilloscope trace showing the light intensity as a function of the time is shown in Fig. 9. The light intensity does not appear to have a square envelope because the signal was obtained from the direct current amplifier output of the photomultiplier microphotometer, which has poor high frequency response. The variation of the light intensity duration, amplitude, and time of arrival behaves as would be expected with variation of the pulse length, pulse amplitude, and transducer to light beam separation.

Waveform distortion in an ultrasonic pulse. In the past decade, special attention has been paid to the distortion of ultrasonic waves by finite amplitude effects. There

is a tendency for finite amplitude waveforms to become somewhat "sawtooth" in shape with propagation for large pressure amplitudes in low-dissipation media. The magnitudes of the harmonic components may be considerable. For example, an initial pressure of only 0.5 atm at 5 Mc in water is theoretically sufficient to give rise to a maximum second harmonic component of 17.6% of the initial fundamental pressure amplitude at a distance of 43 cm, assuming plane waves(8).

Among the methods of experimental investigation which have proven useful are optical techniques, especially light diffraction methods. In general, theories for the diffraction of light by ultrasonic waves take into account the phase modulation of the light wavefronts emerging from the medium. This phase modulation is assumed to be a replica of the ultrasonic waveform in the medium.

These waveforms, in the case of finite-amplitude ultrasonic waves, are asymmetric and give rise to asymmetric light diffraction patterns. These light diffraction patterns have been investigated theoretically and experimentally by Zankel and Hiedemann (38), who were able to predict the light intensity distribution in the diffraction pattern from an assumed ultrasonic waveform.

The equivalence of the finite amplitude waveform obtained with pulses and with continuous waves can be demonstrated by means of the light diffraction patterns obtained in the two cases. The optical work at high intensities is,

in the case of pulses, not hindered by the heating and streaming of the liquid associated with the high average input power of continuous waves. Figures 10 and 11 show light intensities obtained in the positive and negative first diffraction orders with pulses and with continuous waves as a function of transducer voltage (initial pressure) at two distances.

The data for Figs. 10 and 11 were obtained in the following way: The apparatus was aligned as for calibration, but with sufficient propagation distance for the ultrasonic beam to undergo finite amplitude distortion before crossing the light beam. In order to demonstrate this effect, distances of 13 and 23 cm were used so as to obtain waveform, or asymmetry, differences. The frequencies of the pulser and continuous wave source were set to coincidence, and the pulse length adjusted to 11.7 $\mu$ sec. The transducer was the same as was used for the calibration procedure, and the water temperature was 28° $\pm$ 1°C. The data for the curves were then recorded by measuring light intensities as a function of transducer voltage. The values of the light intensity maxima of the plus and minus first orders of diffraction were compared for pulses and continuous waves in order to obtain a scale factor ( $\sim$ 50 in this case), which was used to reduce the continuous-wave light intensities to the same magnitude as the pulse-average light intensities. One sees that the data for pulses and for continuous waves

very nearly coincide. The slight differences can be attributed to experimental error, or to heating and streaming in the case of continuous waves. The curves are very similar to those obtained by Zankel and Hiedemann (38) for the first diffraction orders.

It is easy to obtain large sound-pressure amplitudes in the case of a pulsed ultrasonic beam as compared with a continuous one because of the short period of time that the pulse is on and consequent low average power input. This immediately leads to the possibility of obtaining sound-pressure amplitudes large enough to cause finite amplitude waveform distortion. For example, considerable distortion is evident at the 10-v point on Figs. 10 and 11, but the average acoustic power used at that point was of the order of 2 $mw/cm^2$. It is of interest to note that the method described here should be applicable with an average input power several orders of magnitude smaller.

In the case that large ultrasonic-pressure amplitudes are obtained, one must also exercise care to remain in the region of validity of the Raman-Nath theory for light diffraction. This region has been summarized by Zankel and Hiedemann (38).

## The Fundamental Frequency Component of a Plane, Finite Amplitude Wave

General. The propagation of the fundamental frequency component of a plane, finite amplitude wave is of special importance because it represents a large portion of the energy transported by the wave. In addition, measurements of the absorption coefficient of the fundamental frequency component in the region of stable waveform should characterize the wave as a whole.

It is possible to show that waves of finite amplitude "stabilize," that is, the competing processes of generation and absorption of higher harmonics may reach a stage where they nearly balance, the result being a wave which approximately maintains its Fourier spectrum ratios while traveling (7,44). Such waveforms are called "stable waveforms," and they are characterized by the fact that the decay rates of all of the harmonic components are equal.

In general, a graph of the fundamental frequency component of a plane, finite amplitude wave shows a gradual decrease at first, followed by a region of rapid loss, and a return to a gradual decrease rate. One thus has to deal with an essentially nonexponential absorption, and the "absorption coefficient" must be specified as to the conditions and the region in which it is measured.

Three methods of dealing with the experimental "absorption coefficient" of a finite amplitude wave have been

employed by other investigators, and a certain amount of misunderstanding has resulted. First of all, it is useful to employ the absorption coefficient of a sawtooth wave, which may be assumed to apply to the case of large amplitude waves in their region of stablization, i.e., after the absorption coefficient has reached its maximum. In this case, the absorption coefficient is proportional to the local fundamental pressure amplitude, and is given by Rudnick (45) and Naugolnykh (46) as

$$\alpha_{finite} = \frac{\pi(\frac{B}{A} + 2)\nu P_1(K)}{2 \rho_o c_o^3} \qquad (34)$$

One may also deal with the maximum value to which the absorption coefficient rises, and this is shown by approximate analysis for large amplitudes to be proportional to either the local or the initial fundamental pressure amplitude (7,24); the difference between the two is neglected. As this is a special case of the sawtooth wave, Eq. 34 above may be expected to apply to this case also. However, other investigators have successfully obtained experimental data showing the linear relation between pressure and absorption without specifying where either is measured (26).

In addition, it is possible to deal with the construct of the "average absorption coefficient." In this case, one may deal only with the endpoints of a pressure versus distance curve, and find what absorption coefficient is

effectively present over that given path length. This sort of absorption coefficient may be useful, for example, in examining the gross features of propagation over a fixed distance. It is not clear in the literature where or whether measurements of this quantity have been made, and if so, whether as a function of the initial pressure amplitude or of some local pressure amplitude (17, 19, 20, 24, 26, 46, 47).

In order to clarify the situation, it would be useful to examine the behavior of all the above "absorption coefficients" with careful regard to both their method of measurement and the place of measurement of the pressure amplitude.

Experimental apparatus. The object of the present investigation is to examine the behavior of the fundamental frequency component of a finite amplitude wave by a new method making use of pulse techniques (48). The fundamental frequency component of a pulse traveling in a liquid may be observed by means of a receiving transducer resonant at the fundamental frequency. A block diagram of the electronic apparatus is shown in Fig. 12. A pulse of rectangular envelope and variable amplitude is generated in the pulser and applied to the sending transducer by means of a tuned autotransformer which provides impedance matching. The amplitude of the pulse is observed on a calibrated

oscilloscope. The received signal is decreased in amplitude by a known amount in the decade attenuator, and is then amplified by display on an uncalibrated oscilloscope. Received signal measurements are made by adjusting the decade attenuator to produce a signal of fixed reference level on the uncalibrated oscilloscope. The transducers are 5 mc barium titanate ceramic type; the sending transducer is a 1/2-inch diameter disc, and the receiving transducer is a small chip obtained from a similar disc. The frequency used is 5.65 mc, and the tank is filled with distilled water at a temperature of 28°C. The sending transducer has been calibrated by a pulse optical technique (see "Calibration of a Transducer," page 27). Distance measurements are made by observing the delay time between the sent and received pulses on a radar range calibrator oscilloscope, which is accurate to within .1% of the elapsed time. The pulse speed in water is assumed to be $1.5 \times 10^5$ cm/sec.

A standard procedure for measurement of the fundamental frequency component using this apparatus would involve translating the transducers with respect to one another, taking care to maintain alignment in the sending transducer beam and maintaining the angular orientation of the transducers. A correction for beam spreading could then be applied, and the near field pressure distribution would be observed. However, it may be difficult to maintain the correct alignment and orientation of the transducers while

traversing over long distances; this would result in false readings. In order to eliminate this problem, a fixed distance method was employed which also corrects for beam spreading and smooths the near field pressure distribution.

Experimental results. The fixed distance method consists of aligning the transducers for maximum signal at one distance, and then observing the nonlinearity of signal transmission with increasing sending signal. Fig. 13 shows the result of such observations for several distances. This nonlinearity of transmission is due entirely to the incrase of finite amplitude absorption with increasing sending pressure. Note that there is a definite upper limit to the sound pressure amplitude which can be transmitted over a given distance. In fact, if the pressure is sufficiently great, the received signal may actually decrease while the sending signal increases.

The results of a study of the maximum fundamental pressure amplitude of a finite amplitude wave which can be transmitted across a given distance under the stated experimental conditions are given in Fig. 14. Note that the maximum pressure amplitude increases rapidly for short distances. The maximum pressure possible pressure amplitude, in atm, is found to be numerically equal to $21.6X^{-.80}$ where X is measured in cm. This relation was obtained at 5.65 mc.

The nonlinear transmitter-receiver curves are now converted into variable distance curves in the following

way: for each value of sending pressure there is a data point on the fixed distance curves. Each of these is seen to represent a fraction of the expected received signal according to linear transmission theory. Thus, the fraction of transmission as compared with linear theory multiplied by $e^{-\alpha x}$ for that distance may be taken as the ratio of the local pressure to the initial pressure. If a number of closely spaced fixed distance curves have been taken, a smooth curve against distance will result. In Fig. 15 are shown a number of variable distance curves for various initial pressures constructed in this way. The upper straight line is the $e^{-\alpha x}$ law proposed by linear theory. Note that the absorption coefficient$(1/p)(dp/dx)$ is a rapidly increasing function of the distance, and that it reaches a maximum value at some distance which depends on the initial pressure amplitude of the wave. Due to this behavior of the absorption coefficient, it is seen to be very difficult in the case of large amplitudes to attempt to obtain the initial pressure amplitude by extrapolating pressure versus distance curves to the transducer face.

In order to test the validity of the experimental method, it is proposed to check a few known facts with the data at hand. For example, weak shock theory predicts that the local absorption coefficient for a sawtooth wave is proportional to the local fundamental frequency pressure component. (See Eq. 34.) Tangent lines have been drawn

to the pressure versus distance curves at convenient intervals of a few centimeters, and the local absorption coefficient calculated as a function of the local fundamental pressure component. The result is shown in Fig. 16. Data curves for six different sending pressures have been analyzed, and a straight line of best fit drawn. The value of B/A obtained from the line of best fit is $6.3 \pm .8$ which agrees well with experimentally determined values of B/A by others (26, 49). The line shown for B/A = 5.2 refers to a result obtained by Beyer (31) from theoretical considerations.

The "absorption coefficient" rises to a maximum value at some distance from the transducer. Other experimenters have also found that this maximal absorption coefficient is linear with the initial pressure (26). Since it is also linear with the local pressure, the local pressure at the maximal value of the absorption coefficient must be linear with respect to the initial pressure. Figure 17 shows this linear relationship.

We also find that the average "absorption coefficient" over an interval of distance is proportional to the initial pressure amplitude; see Fig. 18. The space averaged "absorption coefficient" has been calculated for 20, 30, and 50 cm, and is found to be linear with the initial pressure amplitude with a slope which increases with decreasing distance.

## The Second Harmonic Frequency Component

General. The theory presented predicts the Fourier spectrum of the wave, based on the two parameters K and $\alpha L$. Accordingly, a complete verification of the theory would require a variation of all of the constants involved in the parameters, and a verification for all of the significant harmonic components of the wave. However, it is sufficient to measure the second harmonic component as a function of $\alpha L$ and K, since it is the major determination of the departures of the waveform from sinusoidal. It is desirable to use a commonly available, pure liquid whose fluid properties are well known in order to determine the values of the governing parameters as accurately as possible. Water was chosen as the fluid, and the frequency of the waves was taken at 5.0 mc/sec, in order to obtain $\alpha L$ values of a convenient order of magnitude while allowing the use of optical methods.

It is preferable to employ ultrasonic pulse techniques, inasmuch as continuous wave measurements introduce the difficulties of heating and streaming of the liquid at large amplitudes, and require the elimination of standing waves.

Experimental data is desired which gives the harmonic structure of the wave over a range of both the initial value and distance parameters. In the literature one finds that a few measurements have been made over a range of distances, but the available range of initial value parameters is small (see Table IV).

TABLE IV

AVAILABLE $\alpha L$ VALUES

| | |
|---|---|
| Krassilnikov, et al. . . | .011<br>.022<br>.043 |
| Ryan, et al. . . . . | .016<br>.032 |
| Present work . . . . . | .10-1.7 |

For example, good agreement between theory and experiment have been obtained by Ryan, Lutsch, and Beyer (27) for the $\alpha L$ values shown over a range of distances. Also, Keck and Beyer (13) have successfully fitted values of the harmonics obtained by Krassilnikov, Shklovskaya-Kordy and Zarembo (22), and the $\alpha L$ values in this experimental work were of the order of .01 - .04. Since a solution for dissipationless fluids, or the case $\alpha L = 0$ is known exactly, all of the available dissipative theories, which are really approximations for the case $\alpha L$ not zero, add to our knowledge only if they are valid for large values of $\alpha L$. Since none of them has been compared with experiment for values of $\alpha L$ as large as .05, further experimental work is called for in the region $\alpha L > .05$. The experimental work presented below spans the range $\alpha L = .1$ to 1.7, and compares results with theory for the second harmonic in that region over a range of distances.

Experimental arrangement. The electronic apparatus is shown in Fig. 19. A pulser or a continuous wave source,

each set to 5.0 mc, may be chosen by means of a switch. The second harmonic component of the wave is received by a 10 mc barium titanate transducer and passed through a filtered amplifying system so as to display the 10 mc second harmonic frequency component on an oscilloscope. The medium is distilled water; the transducers are in rotating mounts about vertical and horizontal axes to allow for alignment, and can be translated to a separation of 80 cm. The filtered amplifying system is prevented from overloading by means of the decade attenuator, which also provides a test of the linearity of the system while in use. Distance measurements are made by reading the time of traversal of the pulse between the two transducers on a radar range calibrator oscilloscope, which is accurate to about .1% of the elapsed time. The pulse velocity is assumed to be $1.5 \times 10^5$ cm/sec.

The sending transducer is a 1 x 1 inch barium titanate ceramic type, and the receiving transducer is either a 3 x 3 mm or 1/2 x 1/2 inch barium titanate ceramic, depending on the sensitivity required.

Transducer calibration. The receiver-tuned amplifier system for the second harmonic is calibrated in actual use by allowing a wave of known second harmonic component to fall on it, while measuring the actual voltage response of the entire system. Two methods of obtaining a wave of known second harmonic content are used, and both give the same end result.

First of all, at small reduced distances and small amounts of second harmonic, one would expect the simple dissipationless theory to be valid. Then it should be the case that the smallest possible reading of second harmonic content at a given distance is correct, according to dissipationless theory, and this can be used as a calibration-point.

Second of all, it is possible to verify a postulated finite amplitude waveform by observing the light diffracted by such a wave. The asymmetric ultrasonic waveforms in the finite amplitude case give rise to asymmetric light diffraction patterns, and these patterns can be predicted from knowledge of the Fourier spectrum of the wave. A number of light diffraction patterns making use of the theoretical harmonic structure of the wave for one value of the initial value parameter have been computed. In this way, predicted light diffraction patterns have been compared with experimental ones every few cm. By inserting various values for the harmonic structure of the wave in the calculation, it is found that the (n -1)st orders of diffraction are very sensitive to the magnitude of the nth harmonic, at least for n = 1, 2, 3. It is thus comparatively easy to separate the effects of various Fourier components of the wave from each other.

Good agreement was obtained between theory and experiment if the fundamental, second and third harmonics of the wave were considered correct according to the theory for the

case $\alpha L = .370$. This corresponds to an initial pressure amplitude of .5 atm in the case at hand.

One thus has a wave of known absolute second harmonic content which can be used to calibrate the receiver. It is furthermore possible by this means to obtain a superior calibration for the initial transducer pressure. That is, agreement between theory and experiment can be forced by varying the transducer voltage at fixed distance and obtaining a fit between the predicted and observed light diffraction patterns. The voltage so obtained can then be used as a calibration point. By averaging a number of such forced-fit calibrations, a calibration for the initial pressure amplitude can be obtained which has the advantage of compensating for near field pressure fluctuations. The value of the case at hand was found to be .054, $\pm$ .0053 at/volt. This probable error was obtained from an analysis of the deviations of the measurements from the mean. There is an additional possible error of about 10% inherent in any absolute optical calibration caused by a lack of accurate knowledge of the piezo-optic coefficient of water. This calibration is in good agreement with calibrations carried out near the transducer face.

Experimental results. The system comprised of calibrated sending and receiving transducers, with the associated electronic apparatus, could now be used to obtain the second

harmonic component of the wave as a function of the distance by increasing the transducer separation while maintaining alignment. There are several difficulties inherent in this scheme. For example, it is difficult to maintain correct transducer alignment while in the process of moving them. A smoothed plot of the second harmonic of the wave can be obtained by means of the fixed distance method. This method and results obtained by it were described in the section on the fundamental frequency component.

Fixed distance measurements in the present case may be made by aligning the transducer system previously calibrated, and recording the received second harmonic as a function of the initial fundamental pressure amplitude. This can conveniently be correlated with theory by calculating the $\alpha$L and K value for each value of initial pressure at which readings are taken. One can then find the appropriate second harmonic value for the theory by referring to Table II with both $\alpha$L and K variable. In Figs. 20 to 25 one sees the result of such theoretical calculations as the solid line; the experimental data points are seen to agree quite well with the theory. The theory line is shown as far as it applies; that is, as the initial pressure is increased at fixed X, K increases and finally becomes unity. As has been pointed out, the theory applies only for $K \leq 1$ (see Chapter II). The data points are referred to as either "large" or "small," depending on whether the

measurements were made with the large (1/2 x 1/2 inch) or small (3 x 3 mm) receiver.

Such fixed distance measurements allow sufficient correlation with theory to indicate good agreement, but do not give as good an idea of the variation of the second harmonic with distance for fixed initial pressure as one may desire. The fixed distance data may be converted to variable distance data by recording the value of the second harmonic obtained at a given initial pressure for a number of distances. The results of several such data tabulations are shown in Figs. 26 to 29 as graphs of the second harmonic against distance for fixed initial pressure. The soild line shows the theory, and is a straightforward application of the tabulated values, Table II, for fixed $\alpha L$ but variable K, which corresponds to fixed initial pressure. The dotted line is extrapolation of the theory to fit the data points in the region $K > 1$.

In all of the above calculations of K and $\alpha L$, the values $\rho_o = 1.0$ g/cc, $C_o = 1.5 \times 10^5$ cm/sec, $\omega = 5.0 \times 10^6$ CPS, and B/A = 5.0 have been assumed. This results in the relations

$$\alpha L = .185\ P_1(0)^{-1} \tag{35}$$

and

$$L = 30.6\ P_1(0)^{-1}\ \text{cm} \tag{36}$$

where $P_1(0)$ is measured in atm.

# CHAPTER IV

## SUMMARY

The theory which has been presented has, as its foundation, the postulate that the interactions between the harmonic components of a plane, finite amplitude wave are weak compared to the absorption mechanism and the mechanism of higher harmonic formation. This assumption takes the mathematical form that the derivative of the pressure of a given harmonic component of the wave is equal to the sum of the derivatives due to the absorption and generation of higher harmonics separately (Eq. 26). The fact that one is able to thus write an experimentally verified solution of a nonlinear problem free of interaction terms and in a readily calculated form justifies the assumption. In addition, it is clearly seen that the solution is a function of two parameters K and $\alpha$L, so that, for example, one may make use of "scaling" techniques, that is, equal values of K and $\alpha$L in completely different fluids should yield the same harmonic wave structure.

The verification of the theory has been done extensively only for the second harmonic frequency component, but the fundamental and third harmonic components also agree with the predictions of the theory for one value of

$\alpha L = .37$. This verification was not carried out extensively for the fundamental frequency component because of the use of the fixed distance method, which works best for large pressure amplitudes in this case. Since the theory holds only for distances $X \leq L$, and L, for example, is 6cm at 5 atm of initial pressure under these experimental conditions, it would be necessary to make the theory comparisons at very small distances and $\alpha L$ values. The development of the fixed distance method was most useful, in the case of the fundamental frequency component, for studying the absorption coefficient and its implications. Among those implications were the possibility of determining B/A, and the maximum sound pressure amplitude which could be transmitted over a given distance. The fixed distance method proved to be a very sensitive method for the determination of the second harmonic frequency component of the wave, and thus performed well at small values of initial pressure. This allowed a verification of the theory for the second harmonic in a region of interest.

Preliminary to the investigation of the harmonic components of the wave, the development of the tools of investigation was necessary. The extension of the known optical methods of measuring sound pressure amplitudes and waveforms to the case of ultrasonic pulses put the use of pulse methods on a firm basis. The demonstration of the equivalence of both the transducer calibration and the

finite amplitude waveform for the case of pulses and continuous waves made the two interchangeable for the purposes of the investigation. In addition, the results of pulse calibration proved very reliable because of the low average input power and consequent lack of heating and streaming, often a problem in the use of optical methods.

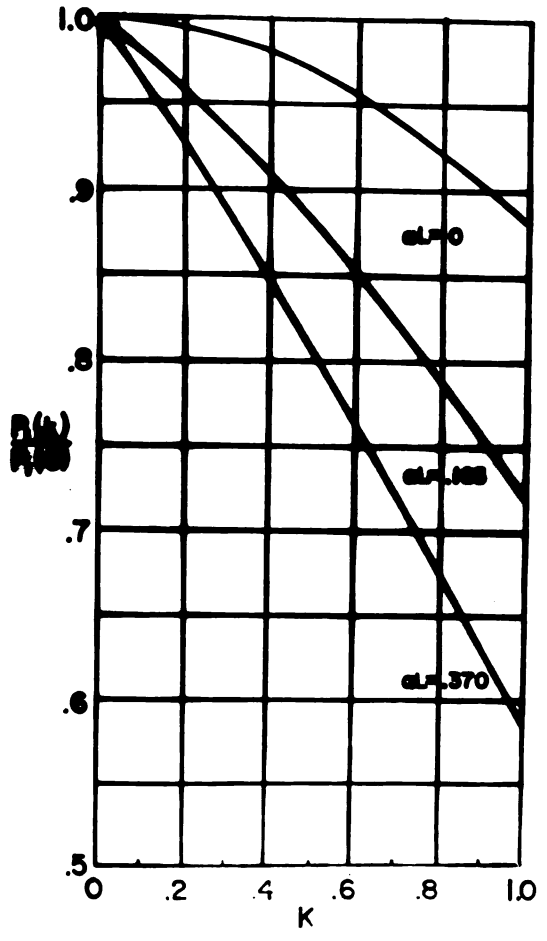


Fig. 1. Fundamental frequency component, in terms of the initial fundamental pressure.

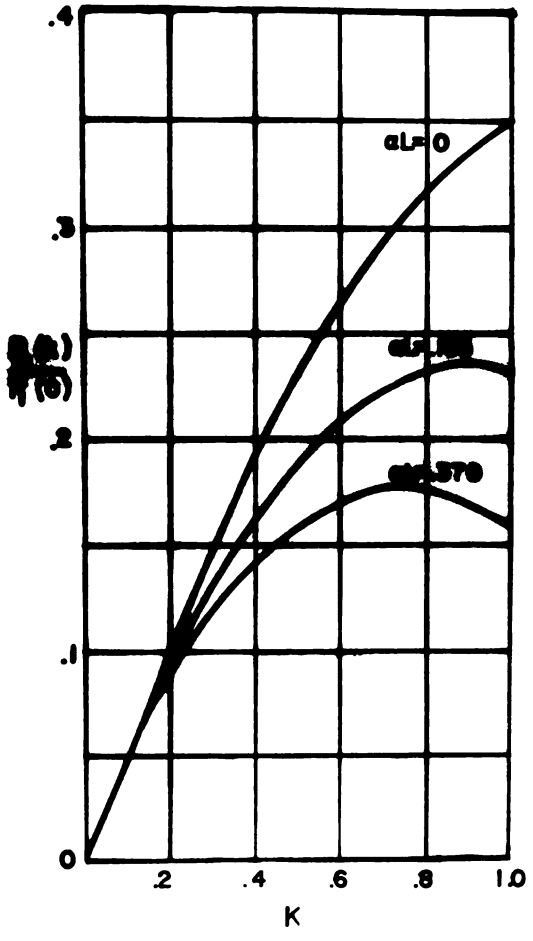


Fig. 2. Second harmonic frequency component, in terms of the initial fundamental pressure.

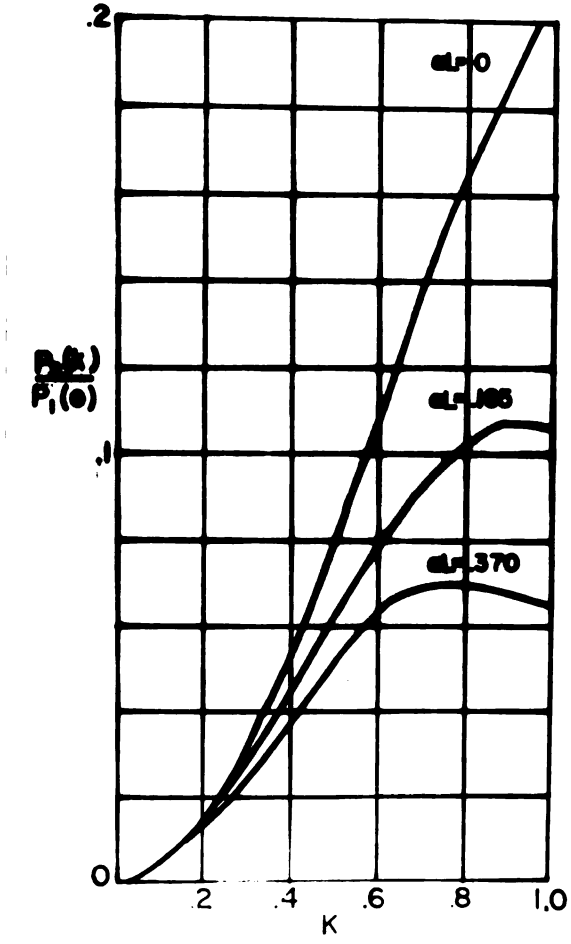


Fig. 3. Third harmonic frequency component, in terms of the initial fundamental pressure.

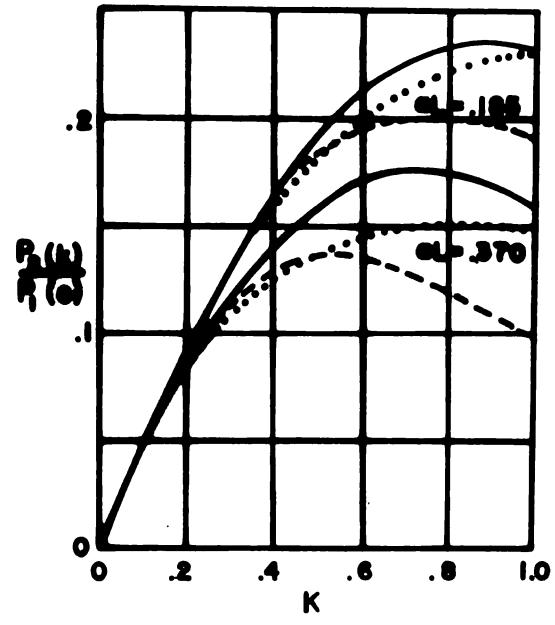


Fig. 4. Second harmonic, as predicted by Fox and Wallace (dashed line), as predicted by Eq. 31 (solid line) and as predicted by Keck and Beyer (dotted line).

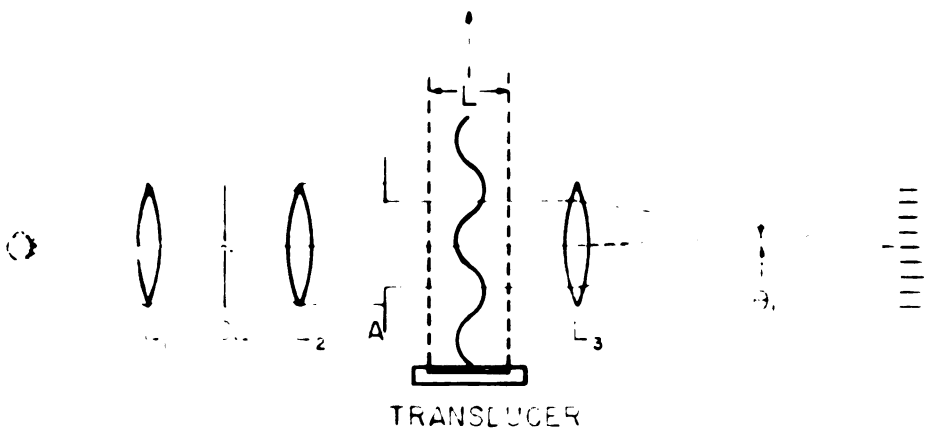


Fig. 5. Optical apparatus for diffraction studies.

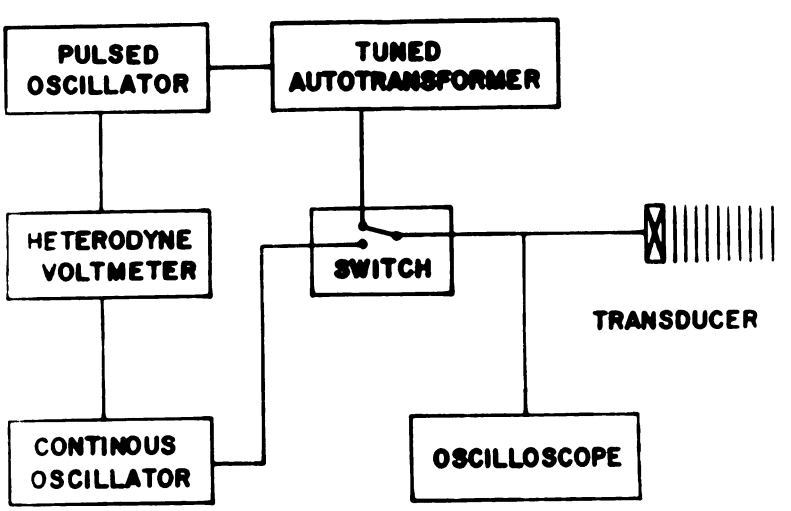


Fig. 6. Electronic apparatus for calibration of a transducer.

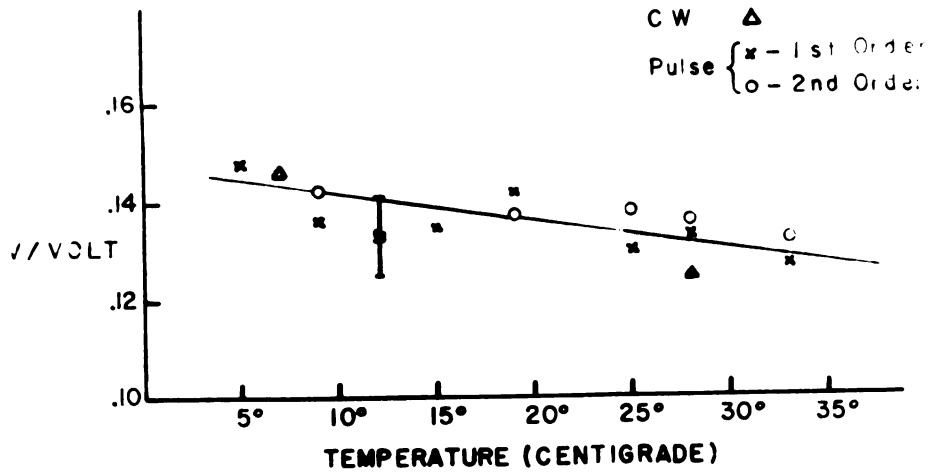


Fig. 7. Raman-Nath parameter per peak-to-peak volt as a function of temperature.

Fig. 8. Oscilloscope traces of the outgoing electrical pulse.

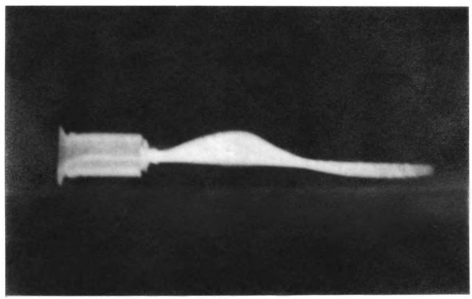

Fig. 9. Oscilloscope trace of the light intensity in the first diffraction order.

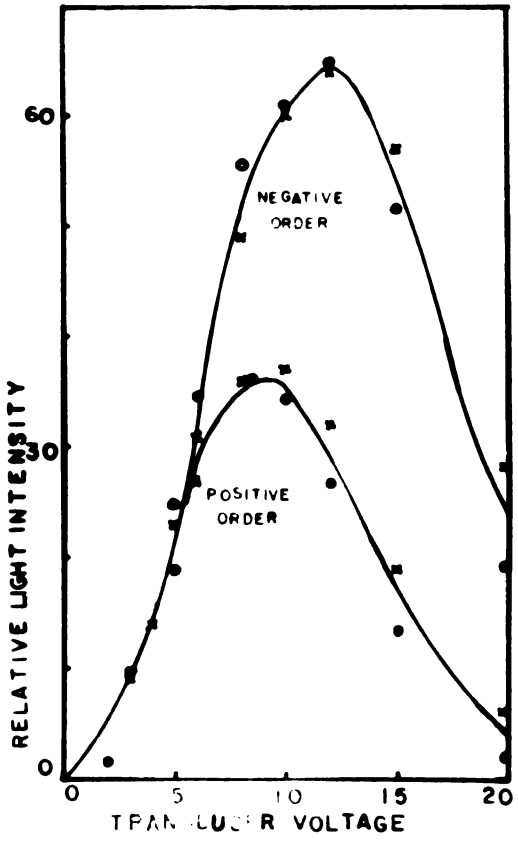


Fig. 10. Normalized first-order diffracted light intensities as a function of initial sound-pressure amplitudes in pulses (crosses) and in continuous waves (circles) at 13 cm.

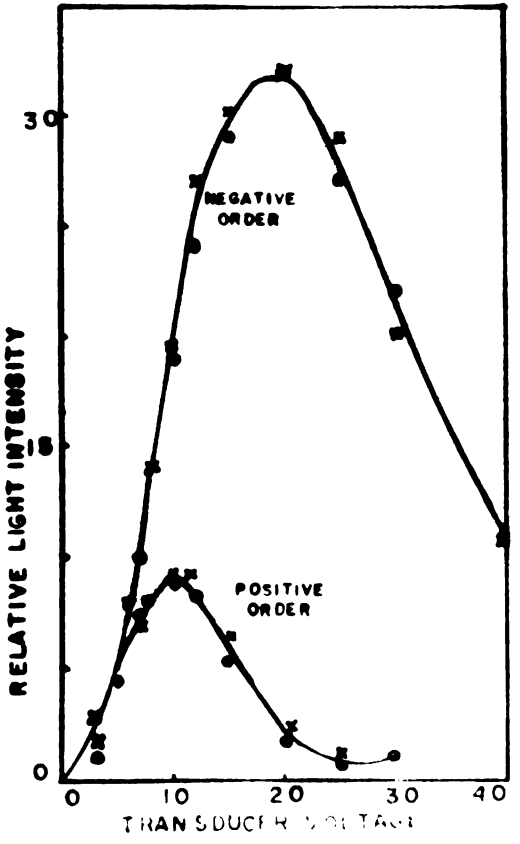


Fig. 11. Normalized first-order diffracted light intensities as a function of initial sound-pressure amplitudes in pulses (crosses) and in continuous waves (circles) at 23 cm.

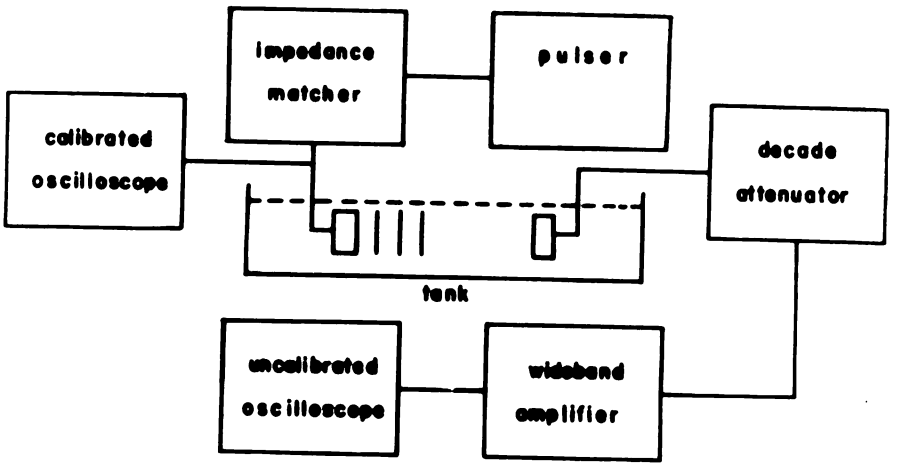


Fig. 12. Electronic apparatus for study of the fundamental frequency component.

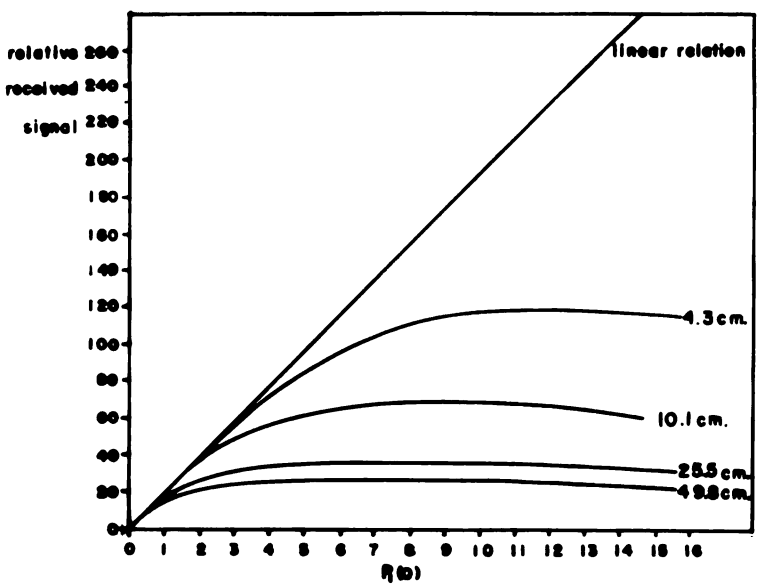


Fig. 13. Relative received fundamental frequency component, as a function of the initial peak pressure amplitude in atmospheres.

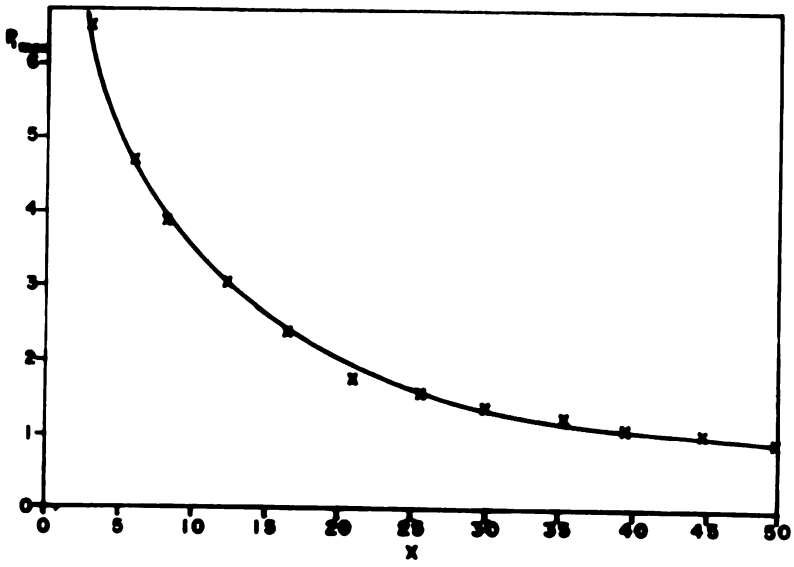


Fig. 14. The maximum amount of fundamental frequency component which can be transmitted over a given distance X.

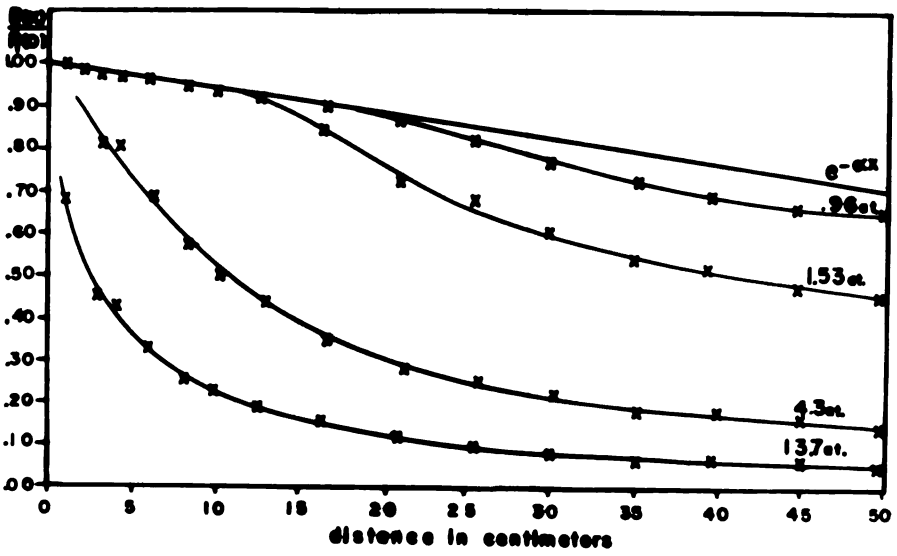


Fig. 15. The fundamental frequency component as a function of the distance, for several initial pressure amplitudes.

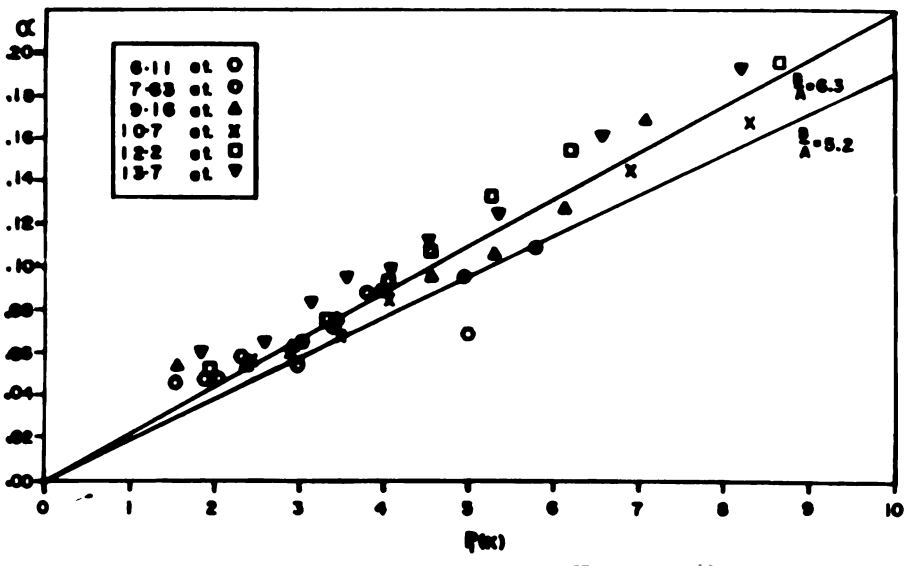


Fig. 16. The local value of the absorption coefficient of the fundamental frequency component as a function of the local pressure.

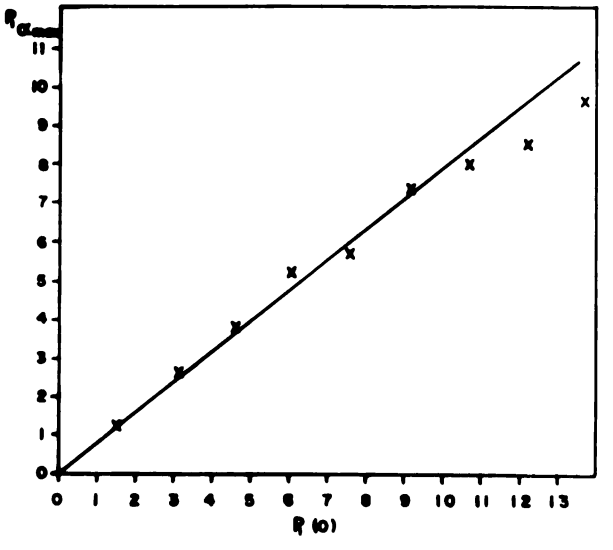


Fig. 17. The pressure, in atm, at which the maximum value of $\alpha$ is observed as a function of the initial peak pressure amplitude in atm.

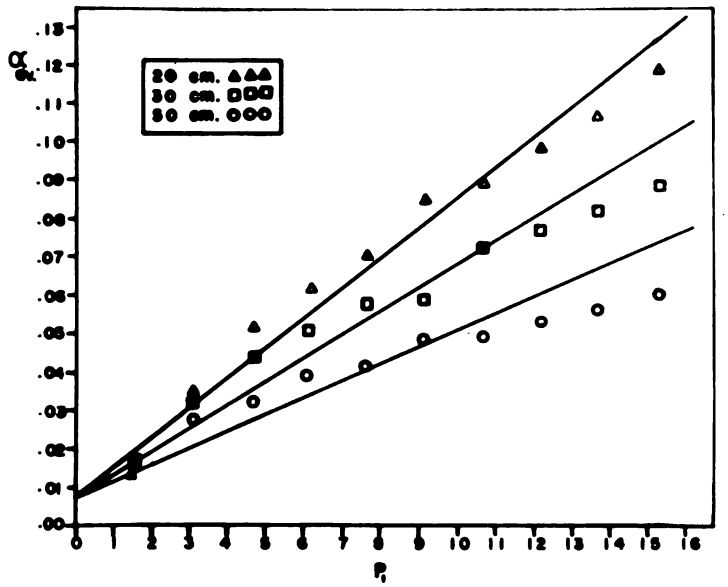


Fig. 18. The average absorption coefficient over a number of fixed paths, as a function of the initial pressure amplitude in atm.

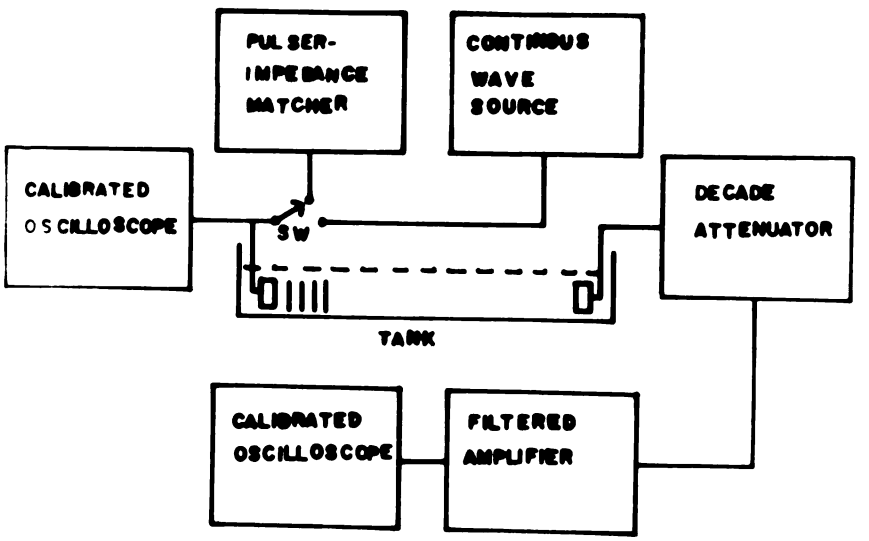


Fig. 19. Electronic apparatus for study of the second harmonic frequency component.

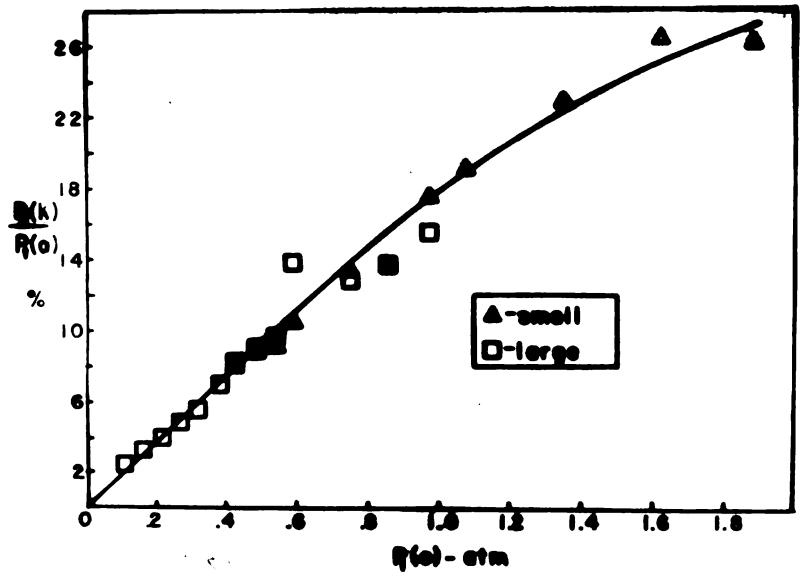


Fig. 20. The second harmonic frequency component as a function of the initial peak pressure amplitude at 13.4 cm. (The solid line is the theoretical prediction.)

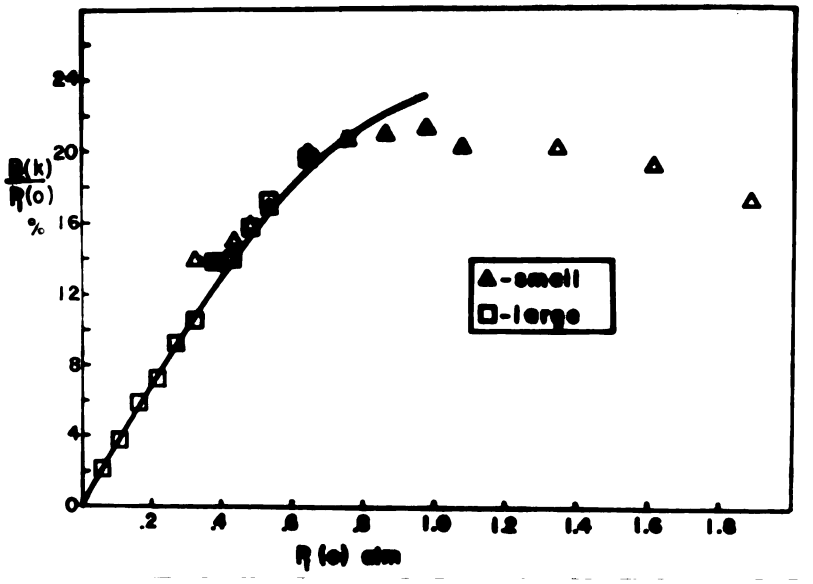


Fig. 21. The second harmonic frequency component as a function of the initial peak pressure amplitude at 30 cm. (The solid line is the theoretical prediction.)

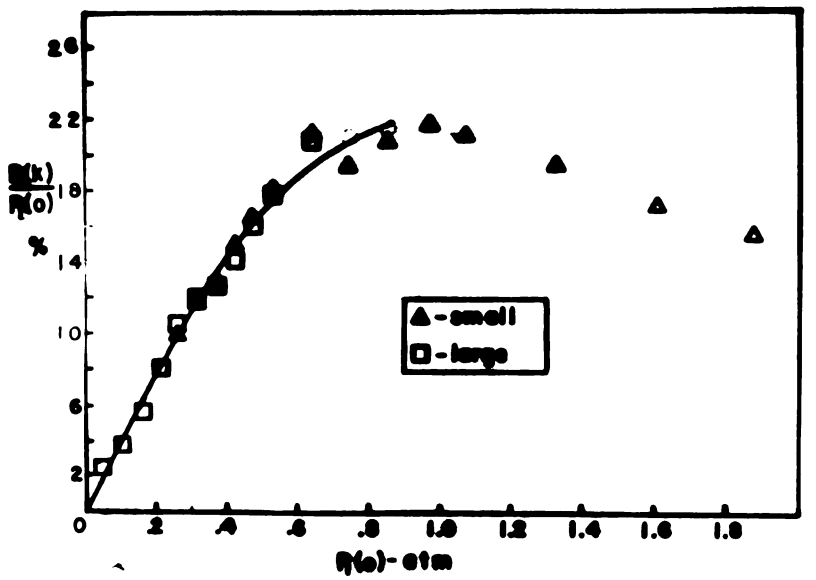


Fig. 22. The second harmonic frequency component as a function of the initial peak pressure amplitude at 35.2 cm. (The solid line is the theoretical prediction.)

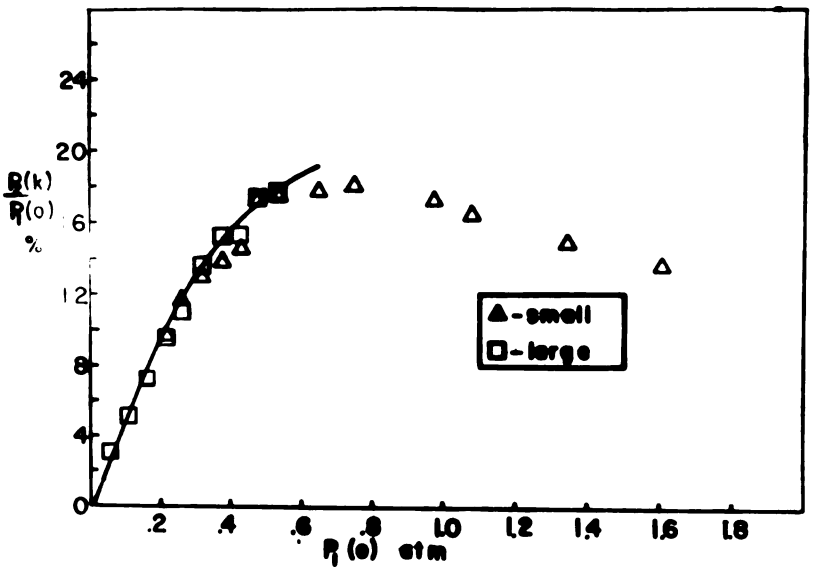


Fig. 23. The second harmonic frequency component as a function of the initial peak pressure amplitude at 48.8 cm. (The soild line is the theoretical prediction.)

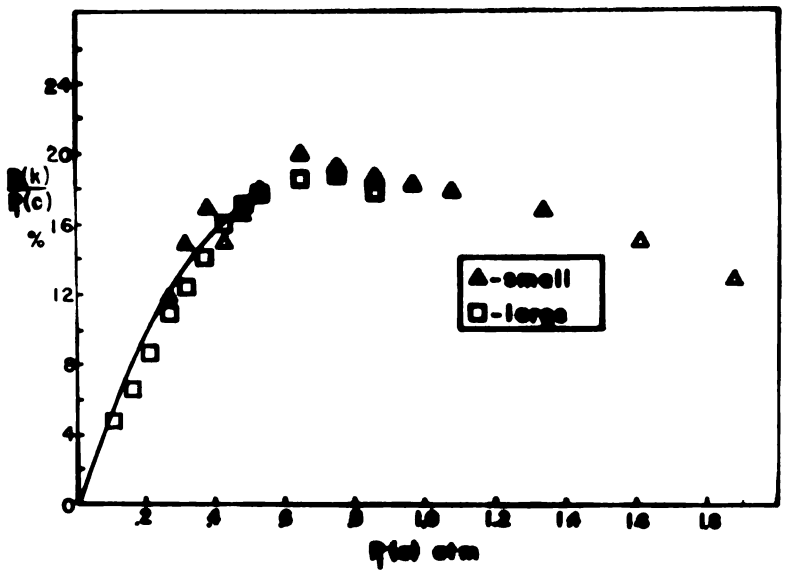


Fig. 24. The second harmonic frequency component as a function of the initial peak pressure amplitude at 55 cm. (The solid line is the theoretical prediction.)

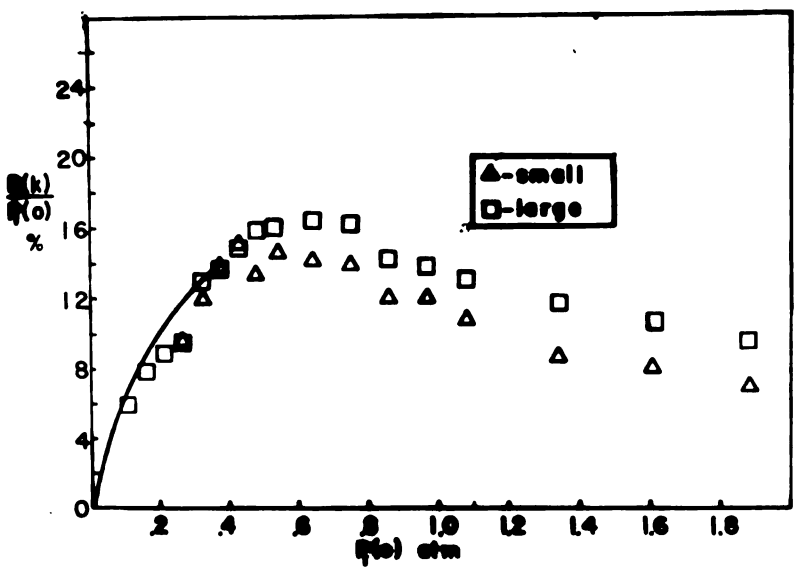


Fig. 25. The second harmonic frequency component as a function of the initial peak pressure amplitude at 80 cm. (The solid line is the theoretical prediction.)

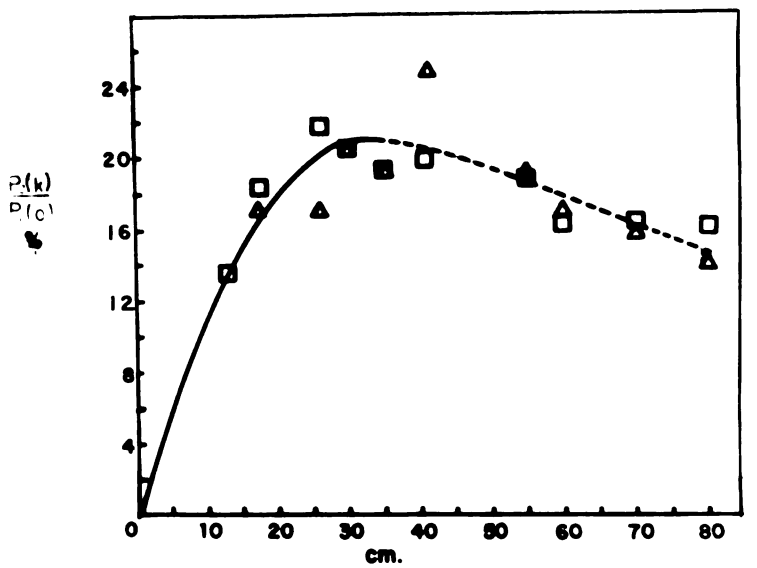


Fig. 26. The second harmonic frequency component as a function of the distance for an initial peak pressure amplitude of .76 atm. (The solid line is the theoretical prediction, and the dashed line, extrapolation.)

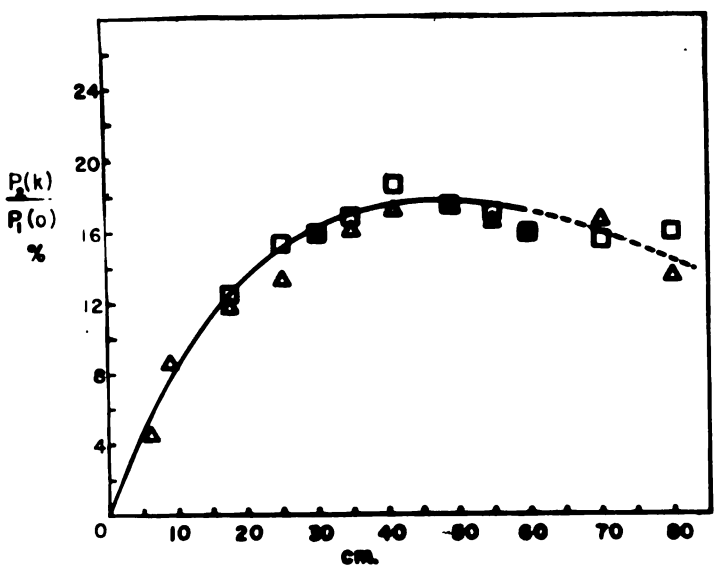


Fig. 27. The second harmonic frequency component as a function of the distance for an initial peak pressure amplitude of .49 atm. (The solid line is the theoretical prediction, and the dashed line, extrapolation.)

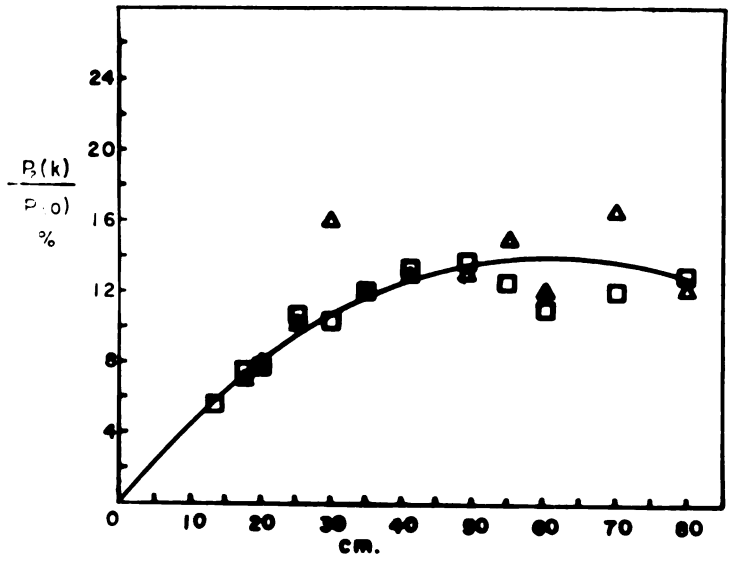


Fig. 28. The second harmonic frequency component as a function of the distance for an initial peak pressure amplitude of .32 atm.

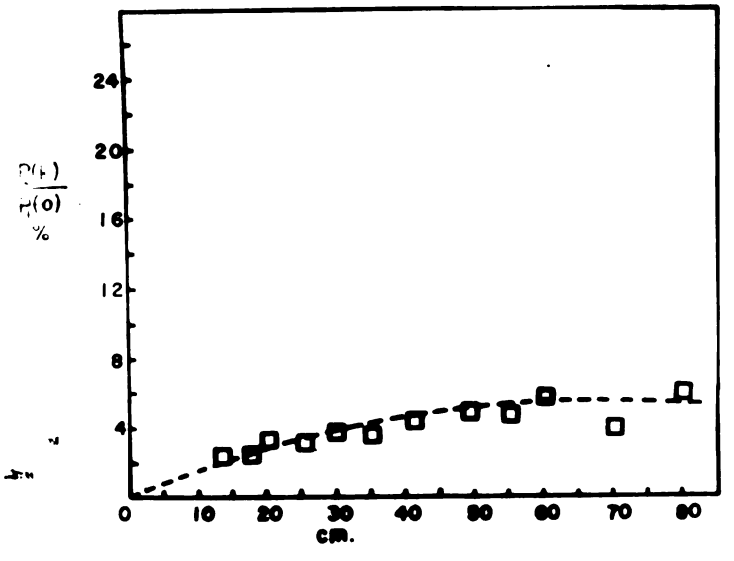


Fig. 29. The second harmonic frequency component as a function of the distance for an initial peak pressure amplitude of .11 atm.

# BIBLIOGRAPHY

## BIBLIOGRAPHY


1. Bernhard Riemann, Gott. Abh. VIII. 43 (1860).
2. Ernshaw, Phil. Trans. cl. 133 (1858).
3. Lord Rayleigh, Proc. Roy. Soc. A, LXXIV. 247 (1910).
4. Lord Rayleigh, Theory of Sound, V. II, Arts. 252 and 253; Dover Publications, New York, 1945.
5. S. D. Poisson, Journ. de L'Ecole Polytechnique, v. 7, 319 (1808).
6. A. L. Thuras, R. T. Jenkins, and H. T. O'Neil, J. Acoust. Soc. Am. 6, 173 (1935).
7. F. E. Fox and W. A. Wallace, J. Acoust. Soc. Am. 26, 994 (1954).
8. William W. Lester, J. Acoust. Soc. Am. 33, 1196 (1961).
9. R. D. Fay, J. Acoust. Soc. Am. 3,222 (1961).
10. Z. A. Gol'dberg, Sov. Phys.-Acoustics 2, 346 (1956).
11. Ibid., 3, 157 (1957).
12. Ibid., 3, 340 (1957).
13. Winfield Keck and Robert T. Beyer, Phys. Fluids 3, 346 (1960).
14. N. N. Andreev, Sov. Phys.-Acoustics 1, 2 (1955).
15. O. Norman Geersten, J. Acoust. Soc. Am. 25, 192A (1953).
16. B. F. Podoshevnikov and B. D. Tartovskii, Sov. Phys.-Acoustics 4, 382 (1958).
17. D. M. Towle and R. B. Lindsay, J. Acoust.Soc. Am. 27, 530 (1955).
18. L. K. Zarembo, V. A. Krassilnikov, and V. V. Shlovskaia-Kordi, Sov. Phys.-Doklady 1, 434 (1956).
19. V. Narasimhan and R. T. Beyer, J. Acoust. Soc. Am. 28, 1233 (1956).

20. R. T. Beyer and V. Narasimhan, J. Acoust. Soc. Am. 29, 532 (1957).

21. L. K. Zarembo, Sov. Phys.-Acoustics 3, 173 (1957).

22. V. A. Krasil'nikov, V. V. Shklovskaia-Kordi, and L. K. Zarembo, J. Acoust. Soc. Am. 29, 642 (1957).

23. L. K. Zarembo, V. A. Krasil'nikov, and V. V. Shklovskaia-Kordi, Sov. Phys.-Acoustics 3, 27 (1957).

24. R. T. Beyer and V. Narasimhan, Sov. Phys.-Acoustics 4, 196 (1958).

25. V. A. Burov and V. A. Krasilnikov, Sov. Phys.-Doklady 4, 190 (1959).

26. L. K. Zarembo and V. A. Krasil'nikov, Sov. Phys. Uspekhi 4, 580 (1959).

27. R. P. Ryan, A. G. Lutsch, and R. T. Beyer, J. Acoust. Soc. Am. 34, 31 (1962).

28. W. W. Lester and E. A. Hiedemann, J. Acoust. Soc. Am. 34, 265 (1962).

29. J. J. Markham, R. T. Beyer, and R. B. Lindsay, Rev. Mod. Phys. 23, 353 (1951).

30. I. Rudnick, J. Acoust. Soc. Am. 30, 564 (1958).

31. Robert T. Beyer, J. Acoust. Soc. Am. 32, 719 (1960).

32. E. Fubini-Ghiron, Alta Frequenza 4, 530 (1935).

33. Logan E. Hargrove, J. Acoust. Soc. Am. 32, 511 (1960).

34. W. V. Lovitt, Linear Integral Equations; Dover Publications, New York, 1950.

35. M. A. Breazeale and E. A. Hiedemann, J. Acoust. Soc. Am. 31, 24 (1959).

36. M. A. Breazeale, L. E. Hargrove, and E. A. Hiedemann, U. S. Navy J. Underwater Acoustics 10, 381 (1960).

37. M. A. Breazeale, B. D. Cook, and E. A. Hiedemann, Naturwissenschaften 22, 537 (1958).

38. K. L. Zankel and E. A. Hiedemann, J. Acoust. Soc. Am. 31, 44 (1959).

39. L. E. Hargrove, K. L. Zankel, and E. A. Hiedemann, J. Acoust. Soc. Am. 31, 1366 (1959).

40. C. V. Raman and N. S. Nagendra Nath, Proc. Indian Acad. Sci. A2, 406 (1935).

41. Ayhan Cilesiz, Rev. Faculte Sciences Univ. Istanbl Sér. C, Tome XX, Fasc. 2, 94 (1955).

42. William W. Lester, J. Acoust. Soc. Am. 33, 857A (1961).

43. Piezotronic Technical Data, Brush Electronics Co., Cleveland, Ohio, 1953.

44. R. D. Fay, J. Acoust. Soc. Am. 3, 222 (1931).

45. I. Rudnick, J. Acoust. Soc. Am. 25, 1012 (1953).

46. K. A. Naugolnykh, Sov. Phys.-Acoustics 4, 115 (1958).

47. L. K. Zarembo, V. A. Krasil'nikov, and V. V. Shklovskaia-Kordi, Doklady Akad. Nauk, SSSR 109, 731 (1956).

48. William W. Lester, J. Acoust. Soc. Am. 34, 1991A (1962).

49. Laszlo Adler and E. A. Hiedemann, J. Acoust. Soc. Am. 34, 410 (1962).